

An X-ray investigation of powerful far-infrared galaxies

K. Iwasawa

Institute of Astronomy, Madingley Road, Cambridge CB3 0HA

ABSTRACT

We present ASCA results on four prototype powerful far-infrared galaxies, Mrk231, Mrk273, Arp220 and NGC6240. The soft X-ray spectra show signatures of thermal emission with temperatures of $(0.5\text{--}1)\times 10^7$ K, which is probably produced in starbursts. Their soft X-ray (0.5–2 keV) luminosities range from 4×10^{40} erg s^{−1} to 7×10^{41} erg s^{−1}. The X-ray properties are examined in the context of a starburst. Evidence for a heavily obscured active nucleus is found in Mrk273 and NGC6240. The ASCA spectra of both galaxies show strong iron K emission line features. The hard X-ray emission (> 3 keV) in NGC6240 is most likely the reflected light of a hidden QSO whose intrinsic luminosity is suspected to be $\sim 10^{45}$ erg s^{−1}, comparable to the far-IR luminosity. The 2–10 keV emission, possibly related to an AGN, is found in Mrk231. The observed 2–10 keV luminosity is only $\sim 2 \times 10^{42}$ erg s^{−1}, and the origin of the hard X-ray emission is uncertain due to the low quality of the present data. No evidence for an AGN is found in Arp220 in the X-ray data. However, the soft X-ray emission originating in a starburst is also as weak as the H α nebula and near-IR continuum despite the large far-IR excess. The possible existence of a powerful but heavily obscured (Compton-thick) AGN is discussed.

Key words:

1 INTRODUCTION

The energy source of a class of powerful far-infrared galaxies (FIRGs), which emit the bulk of their bolometric luminosity in the far-IR domain (Soifer et al 1984; Sanders & Mirabel 1996 and references therein), is still a major issue under debate. The large luminosity ($> 10^{11} L_\odot$) of the IR emission, which is likely due to dust reradiation, is comparable with that of QSOs. The far-IR energy distribution of the prototype FIRGs, NGC6240, Mrk273 and Arp220, is similar to starburst galaxies like M82, unlike the ‘warm’ IRAS colour (e.g., $S_{25}/S_{60} \geq 0.2$) typical of Seyfert galaxies and QSOs (DeGrijp et al 1992).

The optical spectra of the nuclear regions of FIRGs resemble LINER or Seyfert 2s (Sanders et al 1988), but they appear to be weak in X-ray. A search for X-ray sources associated with powerful FIRGs in the HEAO-1 A1 all sky survey data failed to detect any (Rieke 1988). No detectable hard X-rays in the 50–700 keV band for Arp220, Mrk273 and Mrk231 with the Compton Gamma-Ray Observatory (CGRO)–OSSE (Dermer et al 1997) rules out luminous Compton-thin X-ray sources ($N_{\text{H}} < 1 \times 10^{24} \text{ cm}^{-2}$). No detection of strong hard X-ray emission means that X-rays from a central source are attenuated by a heavy obscuration, if AGNs power FIRGs.

On the other hand, various observations suggest that

starbursts play a significant role. Direct evidence for a massive star population has been provided by the detection of near-IR CO bandhead absorption at $2.3\mu\text{m}$, which is produced in the stellar atmospheres of red giants and supergiants (Rieke et al 1980, 1985; Walker, Lebofsky & Rieke 1988; Lester et al 1990; Doyon et al 1994; Ridgway, Wynn-Williams & Becklin et al 1994).

A large (tens kpc scale) extended optical emission-line nebula is often found around FIRGs (Heckman, Armus & Miley 1987; Armus, Heckman & Miley 1990). Studies of the gas kinematics in the nebulae (e.g., split line-profiles) have revealed galactic-scale outflow (‘superwind’, Heckman, Armus & Miley 1990) with velocities of a few hundreds–1000 km s^{−1}. A collection of supernovae (SNe) and stellar winds from massive stars in a nuclear starburst can drive this outflow. The LINER-type excitation of the nebular emission-line gas is consistent with shock-heating by the superwind, which is also expected to produce soft X-rays (Chevalier & Clegg 1985; Tomisaka & Ikeuchi 1988). Some FIRGs show extended soft X-ray emission observed with Einstein Observatory and ROSAT (Fabbiano 1988; Strickland, Ponman & Stevens 1997; Heckman et al 1996; Dahlem et al 1997; Schulz et al 1998; Komossa, Schulz & Greiner 1998). Since this process of generating X-rays is thought to be not very

efficient ($\log(L_X/L_{\text{FIR}}) \sim 10^{-4}$), the X-ray quiet nature of FIRGs would not be surprising.

The weak reddening-corrected luminosity (and small equivalent width) of $\text{Br}\alpha$ and $\text{Br}\gamma$ in some FIRGs (e.g., Arp220) have raised the ‘ionization photon deficit’ problem with a starburst model: ionizing photons predicted from the bolometric luminosity significantly overproduce the near-IR lines observed (DePoy, Becklin & Geballe 1987; Goldader et al 1995; Armus et al 1995; Leitherer & Heckman 1995). Although this has sometimes been claimed as evidence against a starburst model, it essentially means that the major energy source (whether starburst or AGN) is heavily obscured in dust even in the near-IR band. The mid-IR line spectroscopy of powerful FIRGs with the Infrared Space Observatory (ISO) Short Wavelength Spectrometer (SWS) found such a large extinction ($A_V \sim 40-50$) for starburst regions (Lutz et al 1996; Strum et al 1996; Genzel et al 1998), and therefore they favour young starbursts as the primary energy source in FIRGs.

However, the existence of an even more deeply buried AGN is still viable. The intensive starburst in the outer part of an obscuring region may mask AGN activity. The nearby FIRG, NGC4945, for which the mid-IR properties are starburst-like, harbours a variable X-ray source absorbed by $N_{\text{H}} \approx 5 \times 10^{24} \text{ cm}^{-2}$ (Iwasawa et al 1993; Done, Madejski & Smith 1996), implying a heavily obscured Seyfert nucleus. The ASCA data on the prototype powerful FIRG, NGC6240, suggests the presence of a QSO nucleus deeply buried in obscuration (Mitsuda 1995; Kii et al 1997; Iwasawa & Comastri 1998 and see below).

High sensitivity observations in hard X-ray band provides a unique probe to such heavily obscured AGNs. The upper-limits of hard X-ray emission for powerful FIRGs obtained from previous observations (Rieke 1988; Eales & Arnoud 1988; Dermer et al 1997) are still consistent with the hypothesis that the FIRGs contains Compton-thick sources like NGC1068: this classical Seyfert 2 galaxy is believed to harbour a powerful Seyfert 1 nucleus behind an obscuring torus (e.g., Antonucci & Miller 1985; Miller, Goodrich & Mathews 1991). The observed hard X-rays are only due to weak reflected light of the central source, whose direct radiation is completely blocked by an extremely thick absorber ($N_{\text{H}} \gg 10^{25} \text{ cm}^{-2}$, Koyama et al 1989; Matt et al 1997) in the line of sight. It should be noted that the hard X-ray flux level is three orders of magnitude below the far-IR emission, which implies the detection limits of HEAO-1 and OSSE are insufficient for distant FIRGs. This classic example makes a sensitive X-ray survey of the FIRGs searching for AGNs still worthwhile.

The Compton-thick situation can be more likely in FIRGs than normal Seyfert 2 galaxies. The large amount of molecular gas concentrated in the central region (sub-kilo parsec in size) of powerful FIRGs (Sanders, Scoville & Soifer 1991; Scoville et al 1991; Solomon, Downes & Radford 1992) and its high density ($\sim 10^4 - 10^5 \text{ cm}^{-3}$, Solomon et al 1992; Bryant & Scoville 1996; Scoville, Yun & Bryant 1997) would easily make up a large column density (e.g., $> 10^{24} \text{ cm}^{-2}$) to suppress the direct X-ray radiation from a central source.

Even reflected light would be difficult to detect in the soft X-ray band as observed with ROSAT, since moderate absorption ($\sim 10^{22} \text{ cm}^{-2}$) would be expected because of the high extinction for the nuclear regions, and it suppresses the

soft X-ray light. Therefore X-ray observations above $\sim 2 \text{ keV}$ are important to observe AGN free from absorption.

The reflection-dominated X-ray spectrum is characterized by a flat hard X-ray continuum and a strong iron K line at 6.4 keV, as seen in NGC1068 (Marshall et al 1993; Ueno et al 1994; Iwasawa, Fabian & Matt 1997). Therefore X-ray spectra are also important to assess the origin of observed X-ray emission.

Using good spectral resolution and high sensitivity to X-rays above 2 keV, where AGN emission would dominate, we study four prototype powerful FIRGs, Mrk231, Mrk273, Arp220 and NGC6240. We discuss the implications on starbursts and AGNs from the X-ray data, and the primary energy sources of the FIRGs.

2 SELECTED SAMPLE

We present results on four prototype powerful FIRGs: Arp220, NGC6240, Mrk231 and Mrk273 (Table 1). They are all among the infrared colour-selected sample (ICSS) galaxies (Armus, Heckman & Miley 1990) and lie in a well-defined part of IRAS colour-colour diagram ($\alpha_{25-60} < -1.5$, $\alpha_{60-100} > -0.5$) which is distinctive from where other class of objects occur: their ‘tepid’ characteristic temperatures are different from that of normal galaxies or Seyferts/QSO. The four galaxies are good representative of the particular class of objects in terms of large IR luminosity ($\sim 10^{12} L_{\odot}$), characteristic far-IR spectrum, distorted host galaxy, and concentrated large molecular gas content ($M_{\text{H}_2} \geq 10^9 M_{\odot}$, Sanders, Scoville & Soifer 1991; Scoville et al 1991). A double nucleus is found in all galaxies except Mrk231. The optical spectra of their nuclear regions are considerably red and the emission-line properties are classified as LINER (NGC6240) Seyfert-2 (Mrk273 and Arp220) and Seyfert-1 (Mrk231). Kinematic signatures of galactic-scale outflow (e.g., split line profiles, Heckman et al 1990; Hamilton & Keel 1987) have been found in the circumnuclear regions, and large extended $\text{H}\alpha$ nebulae (tens kpc) were imaged for all the galaxies by Armus et al (1990). Weak soft X-ray emission has been detected from all the galaxies with Einstein Observatory and ROSAT. No detection of X-rays above $\sim 3 \text{ keV}$ has been reported for them before the ASCA observations.

3 OBSERVATIONS AND DATA ANALYSIS

ASCA observations of the sample FIRGs are summarized in Table 2. The data were retrieved from the ASCA archive database maintained by ASCA Guest Observaer Facility (GOF) at Goddard Space Flight Center. Standard calibration and data reduction technique (FTOOLS) are used. Spectral analysis was performed using XSPEC.

ASCA carries four X-ray telescopes (XRT) with focal plane detectors for each (Tanaka, Inoue & Holt 1994). At the moderate spatial resolution of the ASCA XRT (a half power diameter ~ 3 arcmin, Serlemitsos et al 1995) extended X-ray emission from the sample galaxies reported by ROSAT PSPC/HRI observations cannot be resolved.

There are two types of focal plane detectors (a brief description is in Tanaka et al 1994). The Solid state Imaging Spectrometer (SIS; S0 and S1) is an X-ray sensitive CCD

Table 1. The observed sample. The distances to the galaxies are calculated, assuming $H_0 = 75 \text{ km s}^{-1} \text{ Mpc}^{-1}$. The infrared luminosity, L_{IR} , for 8–1000 μm is taken from Soifer et al (1987), which is based on the IRAS fluxes. S_{60}/S_{25} is the ratio of flux densities between 60 μm and 25 μm , measured by IRAS.

Galaxy	IRAS number	z	Distance Mpc	$\log(L_{\text{IR}}/L_{\odot})$	L_{FIR}/L_{\odot}	S_{60}/S_{25}
Mrk 231	12540+5708	0.042	174	12.50	20	4.6
Mrk 273	13428+5608	0.038	152	12.10	29	3.7
Arp 220	15327+2340	0.018	73	12.11	150	13.1
NGC 6240	16504+5235	0.024	100	11.77	45	6.6

Table 2. ASCA observations. * This is the S1 exposure time while 12 ks for S0. The count rates are corrected for background.

Galaxy	Date	SIS mode	Exposure (SIS/GIS) 10^3 s	Count rate (S0/G2) $10^{-2} \text{ ct s}^{-1}$
Mrk 231	1994 Dec 05	Faint+Bright/2CCD	25/21	1.0/0.7
Mrk 273	1994 Dec 27	Faint/1CCD	46/41	1.2/0.7
Arp 220	1993 Jul 26	Faint/1CCD	26*/32	1.0/0.5
NGC 6240	1994 Mar 27	Faint/2CCD	39/41	4.9/2.8

detector (0.4–10 keV band) with higher spectral and spatial resolutions than the Gas Imaging Spectrometers (GIS; G2 and G3 for the 0.7–10 keV band). The higher sensitivity of the SIS to soft X-rays (< 2 keV), combined with the spectral resolution, is suitable to study thermal emission with a temperature of $\sim 10^7 \text{ K}$, often associated to starburst while the GIS has a larger effective area above 5 keV which is useful to detect hard X-ray emission originating in AGN.

The thermal emission model for optically-thin, collisional ionization equilibrium plasma, MEKAL, is used in the spectral fits, with solar abundances by Feldman (1992). The absorption cross sections are taken from Morrison & McCammon (1983). The column densities of Galactic absorption for each galaxy are derived from the HI measurements by Dickey & Lockman (1990). Quoted errors to best-fit spectral parameters are 90 per cent confidence regions for one parameter of interest. The Hubble constant of $H_0 = 75 \text{ km s}^{-1} \text{ Mpc}^{-1}$ is used in deriving distances of galaxies (Table 1).

4 RESULTS

4.1 Mrk231

This galaxy has a single nucleus, although a faint double tidal-tail in the visual image suggests that this system could be a recently completed merger (Huchings & Neff 1987; Sanders et al 1988). The second nucleus claimed by Armus et al (1994) appears to be star-forming knots resolved in the HST image (Surace et al 1998). Besides its large infrared luminosity, Mrk231 has many other outstanding properties. AGN-like phenomena dominate the radio, optical and near-IR band, but the nature appears to be unusual. The optical spectrum of the nucleus shows broad (FWHM $\approx 4200 \text{ km s}^{-1}$) Balmer lines, strong FeII emission and several absorption line systems blueshifted by up to 8240 km s^{-1} (Boksenberg et al 1977). The multiple transitions of FeII emission dominate the optical spectrum while there is little evidence for narrow emission lines. The nonthermal ra-

dio continuum of Mrk231 is variable on time scales of months or years (e.g., Condon, Frayer & Broderick 1991).

The optical continuum of the Seyfert 1 nucleus is considerably red (Weedman 1973; Boksenberg et al 1977). This trend continues to the UV band but with a blue continuum upturn shortward of 2400 \AA probably due to a hot star cluster (Smith et al 1995). Unusually high, wavelength dependent optical/UV polarization (10–20 per cent at shorter wavelengths than 4000 \AA , Thompson et al 1980; Schmidt & Miller 1985; Smith et al 1995) is likely to arise in dust scattering with dilution by the starlight observed in UV. The polarization degree changing across the broad H α profile indicates that some of the broad component is dust-scattered (Smith et al 1995). Various observations suggest that the active nucleus is a BAL QSO, which is mostly obscured by dust and low-ionization gas (e.g., Hamilton & Keel 1987; Smith et al 1995), with strong FeII emission.

However, the type-1 AGN characteristics disappear in the mid-IR and X-ray bands. No high excitation lines were detected in the ISO/SWS spectrum (Rigopoulou et al 1998). Hard X-ray emission is also very faint (< $6.5 \times 10^{-12} \text{ erg cm}^{-2} \text{ s}^{-1}$, Rieke 1988). Since the nuclear absorption ($N_{\text{H}} \sim 4 \times 10^{21} \text{ cm}^{-2}$) implied from the optical reddening ($A_{\text{V}} \sim 2$, Boksenberg et al 1977) should be no longer opaque to X-rays of energies above 2 keV, the lack of detection of strong hard X-rays is puzzling for Seyfert-1/QSO nuclei.

It is interesting to note that estimates of reddening towards the mid-IR nucleus are much larger than that deduced for the optical continuum: $A_{\text{V}} \sim 20$ from the silicate absorption feature at 10 μm (Roche, Aitken & Whitmore 1983); and $A_{\text{V}} \sim 40$ from the [SIII] line ratio (18.7 μm and 33.5 μm , Rigopoulou et al 1998).

Weak soft X-rays have been detected with the ROSAT PSPC. Although Rigopoulou, Lawrence & Rowan-Robinson (1996), Rush et al (1996) and Wang, Brinkmann & Bergeron (1996) fitted the PSPC spectrum with a power-law or bremsstrahlung models, we have found that thermal emission from optically thin plasma, expected from a starburst, is a likely explanation (see below and Table 3). At a temperature around 10^7 K , an X-ray spectrum is of an emission-line dominated regime so a bremsstrahlung model is not appro-

Table 3. Spectral fits to the ROSAT PSPC data on Mrk231. Galactic absorption, $N_{\text{H}} = 1.26 \times 10^{20} \text{ cm}^{-2}$ is assumed for both model. (1) Photon-index of power-law; (2) excess absorption above the Galactic value; (4) temperature of MEKAL thermal emission spectrum; (5) metal abundance.

Power-law		
(1) Γ	(2) N_{H} 10^{20} cm^{-2}	(3) χ^2/dof
1.73 ± 0.15	—	36.82/21
2.22 ± 0.48	2.4 ± 2.0	33.22/20
Thermal emission		
(4) kT keV	(5) Z Z_{\odot}	(6) χ^2/dof
$0.88^{+0.27}_{-0.17}$	$0.10^{+0.08}_{-0.04}$	19.68/20

priate for it. The evidence for thermal X-ray emission is confirmed by the ASCA data. Above the ROSAT band, we detect hard X-ray emission in the ASCA data.

4.1.1 The ROSAT PSPC data

Mrk231 was observed with the ROSAT PSPC on 1991 June 7–8. The energy spectrum of the 24 ks ROSAT PSPC data is reanalysed. Fitting with an absorbed power-law model to the 0.2–2 keV data gives a photon-index of 2.22 ± 0.48 plus intrinsic absorption of $N_{\text{H}} = (2.4 \pm 2.0) \times 10^{20} \text{ cm}^{-2}$, which are consistent with results by Rigopoulou et al (1996). This fit leaves significant residuals around 0.9 keV, which is possibly an emission-line bump due to Fe L. The thermal emission model gives a much better fit (see Table 3) with a temperature of $kT = 0.88^{+0.27}_{-0.17}$ keV and abundance, $Z = 0.10^{+0.08}_{-0.04} Z_{\odot}$. No significant absorption excess above Galactic value is required. The 0.1–2 keV flux estimated from the thermal model is $1.27 \times 10^{-13} \text{ erg cm}^{-2} \text{ s}^{-1}$.

4.1.2 The ASCA data

The signal-to-noise of the ASCA data is rather poor because of the short exposure time for this faint X-ray source. As we showed above for the ROSAT PSPC data, the soft X-ray emission appears to be thermal emission. The soft portion of the ASCA spectrum also indicates a possible Fe L emission peak around 0.9 keV and is described well with the thermal emission model.

We find a hard-spectrum component as well as the thermal emission in the ASCA data (see Fig 1). When the data above 2 keV from four detectors are fitted by a power-law modified only by Galactic absorption ($N_{\text{H}} = 1.26 \times 10^{20} \text{ cm}^{-2}$), a photon index of $0.8^{+0.4}_{-0.5}$ is obtained. This very hard X-ray spectrum above 2 keV is unusual for Seyfert 1 galaxies which generally have photon indices around 1.8 in the ASCA band (e.g., Reynolds 1997). If the hard-spectrum component originates in a central source of the Seyfert 1 nucleus, it could have been altered by absorption and/or reflection.

The whole ASCA spectrum is modelled by a thermal emission model plus an absorbed power-law. The photon index of the power-law cannot be well constrained when it

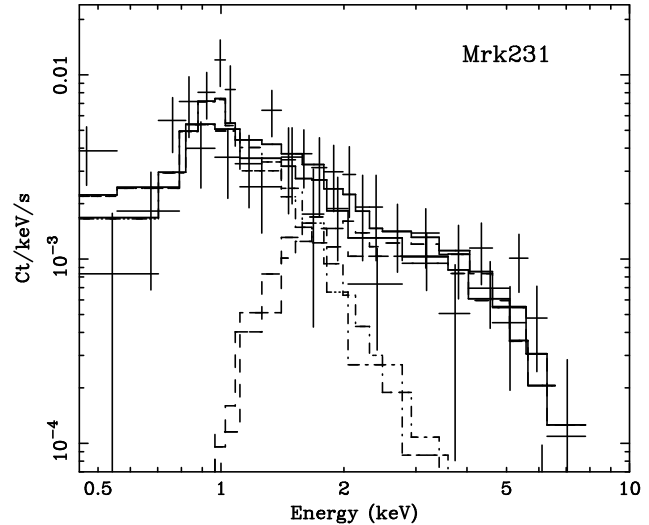


Figure 1. The ASCA SIS spectrum of Mrk231. The data were fitted by a thermal spectrum plus an absorbed power-law. Best-fit parameters are given in Table 4.

is left to be a free parameter (Table 4), $\Gamma = 1.8$, the mean ASCA value for Seyfert 1 galaxies, is also consistent. Results are summarized in Table 4. The temperature and metallicity of the thermal emission model obtained are consistent with the ROSAT results, within the uncertainties. The hard X-ray component can be approximated by an absorbed power-law which has large absorption with a column density of $N_{\text{H}} \simeq 4 \times 10^{22} \text{ cm}^{-2}$, when the $\Gamma = 1.8$ power-law continuum is assumed. As shown above, a flat continuum ($\Gamma \sim 0.8$) with smaller absorption is also acceptable.

The observed total fluxes in the 0.5–2 keV and 2–10 keV bands are $1.2 \times 10^{-13} \text{ erg cm}^{-2} \text{ s}^{-1}$ and $6 \times 10^{-13} \text{ erg cm}^{-2} \text{ s}^{-1}$, respectively. Using the best-fit spectral model, the 0.5–2 keV luminosity of the thermal emission is $4 \times 10^{41} \text{ erg s}^{-1}$, and the absorption corrected 2–10 keV luminosity of the power-law is $2.2 \times 10^{42} \text{ erg s}^{-1}$.

The flat spectrum in the hard X-ray band (> 3 keV) is also consistent with a reflection-dominated spectrum. In this case, a strong iron K line feature would be observed on top of a very flat continuum, like NGC1068 and NGC6240. Unfortunately, the poor signal-to-noise of the present data can provide only a loose constraint on an iron line strength; the 90 per cent upper limit on EW for a narrow line at 6.4 keV is about 0.9 keV.

One might consider the possibility that the observed entire spectrum can be explained by a power-law continuum of the Seyfert nucleus modified by the multiple low-ionization absorption systems observed in the optical band which could impose absorption edges due to partially ionized oxygen [OVII(0.74 keV) and OVIII(0.87 keV)] onto the power-law continuum. However, this possibility can be ruled out. The inclusion of an absorption edge into a power-law to account for the spectral break between 1 and 2 keV seen in the ASCA data however gives a significantly worse fit to the thermal and power-law composite model ($\Delta\chi^2 \sim 11$). The obtained edge energy (1.06 ± 0.05 keV) is too high to match any blueshifted oxygen edges expected from known absorption systems.

Table 4. Spectral fits to the ASCA data on Mrk231 and Arp220. Spectral fittings were performed to the four detectors jointly with a model consisting a thermal emission spectrum and an absorbed power-law. No extra absorption above Galactic extinction ($N_{\text{H}} = 1.3 \times 10^{20} \text{ cm}^{-2}$ for Mrk231 and $N_{\text{H}} = 3.7 \times 10^{20} \text{ cm}^{-2}$ for Arp220) is assumed for the thermal emission component. *: normalization of the thermal emission model in $[10^{-18}/(4\pi D^2)] \int n^2 dV$, where D is the distance of the source and n is electron density in cm^{-3} . †: Normalization of power-law at 1 keV in unit of $10^{-5} \text{ photons keV}^{-1} \text{ cm}^{-2} \text{ s}^{-1}$. Note that the Arp220 data include the southern source (see text).

Galaxy	Thermal emission			Γ	Power-law		χ^2/dof
	kT keV	Z Z_{\odot}	A_{th} *		A_{PL} †	N_{H} 10^{22} cm^{-2}	
Mrk 231	$0.98^{+0.51}_{-0.09}$	$0.08^{+0.2}_{-0.05}$	2.8	$1.2^{+0.7}_{-0.5}$	6.6	$2.1^{+2.5}_{-1.5}$	98.07/116
	$0.98^{+0.66}_{-0.25}$	$0.06^{+0.2}_{-0.04}$	3.2	1.8	18	$3.9^{+3.6}_{-0.9}$	100.2/117
Arp220	$0.76^{+0.11}_{-0.11}$	$0.31 (\geq 0.1)$	0.8	1.8	0.4	$0.8 (< 2.7)$	69.72/69

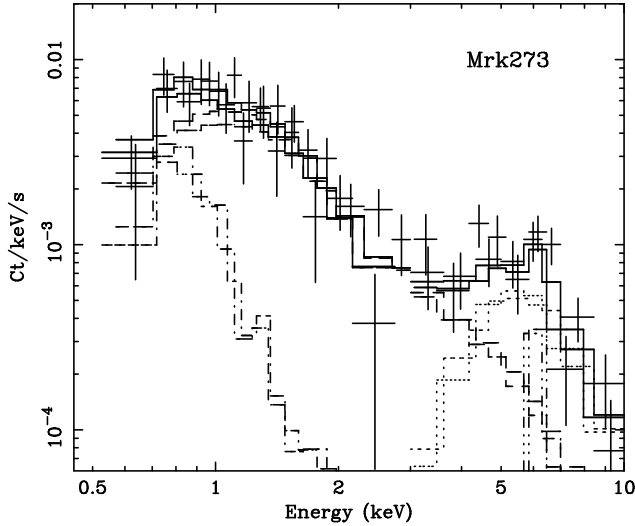


Figure 2. The ASCA spectrum of Mrk273. The data were fitted with a two-temperature thermal spectrum, absorbed power-law plus a gaussian line for the Fe K.

4.2 Mrk273

Mrk273 shows a highly distorted optical morphology with a ~ 1 arcmin-long tail to the south and a multiple core (e.g., Sanders et al 1988). Radio and near-IR imagings show a double nucleus clearly (Condon et al 1991; Majewski et al 1993; Knappen et al 1997). Note that the SE source resolved by Condon et al (1991) may be a background radio source while a weaker SW source associated with the secondary near-IR/optical peak has been found (Knappen et al 1997). The nuclear optical spectrum resembles that of a Seyfert 2 nucleus ($[\text{OIII}]\lambda 5007/\text{H}\beta \sim 10$ and emission-line width of $\text{FWHM} \sim 700 \text{ km s}^{-1}$) with a heavy reddening implied by a large Balmer decrement ($A_V \sim 3$, Koski et al 1978).

4.2.1 The X-ray companion source

A weak soft X-ray source ($f_{0.1-2\text{keV}} \sim 1 \times 10^{-13} \text{ erg cm}^{-2} \text{ s}^{-1}$) has been detected with ROSAT (Turner, Urry & Mushotzky 1993). An X-ray companion source with comparable X-ray brightness was also found at 1.3 arcmin NE of Mrk273 (Turner et al 1993), which has been identified with a dwarf galaxy with Seyfert-2 emission-line characteristics lying at the same red-

shift (Xia et al 1998). In the 0.5–2 keV image of the SIS, the companion source appears to be fainter (at most 40 per cent of Mrk273 in count rate). According to the spectral studies of the ROSAT PSPC data (Turner et al 1993; Xia et al 1998), the companion source has a spectrum similar to or slightly harder than that of Mrk273. Therefore the relatively better efficiency towards 2 keV of the SIS compared with the PSPC cannot be the explanation for the apparent weakness of the companion source during the ASCA observation. All the ROSAT PSPC and HRI observations of Mrk273 were carried out between 1992 May and June. The companion X-ray source has probably faded by factor of 2 or more in 2.5 yr. There is a possible extent to the NW of Mrk273 which was not seen by the PSPC or HRI images.

The brightest source is found at the same position both in the 0.6–3 keV and 4–10 keV images. The data used for spectral analysis were taken from a circular region with a radius of 3 arcmin which also contains the dwarf galaxy. The X-ray fluxes observed with the ASCA SIS are $1.7 \times 10^{-13} \text{ erg cm}^{-2} \text{ s}^{-1}$ in the 0.5–2 keV band and $7.0 \times 10^{-13} \text{ erg cm}^{-2} \text{ s}^{-1}$ in the 2–10 keV band.

4.2.2 The ASCA spectrum

The ASCA spectrum of Mrk273 (Fig. 2) is complex, as seen in classical Seyfert 2 galaxies. Below 3 keV, the SIS spectrum can be roughly described with a power-law with photon-index of ~ 2.4 modified by absorption of $N_{\text{H}} \sim 1 \times 10^{21} \text{ cm}^{-2}$ ($\chi^2 = 42.60$ for 53 degrees of freedom). Although the data are noisy, systematic line-like residuals around 0.7–0.8 keV remain after the fit, which is probably attributed to Fe L emission. If the Fe L emission originates in thermal emission, the temperature of the gas would be $kT \sim 0.4$ –0.5 keV, which is too low to explain the observed spectrum up to 3 keV. Therefore it is plausible that the 0.4–3 keV spectrum consists of low temperature ($kT \sim 0.4$ keV) thermal emission and either power-law or high temperature thermal emission. It is unlikely that the whole soft X-ray emission is scattered light of an AGN, because the optical reddening, $A_V \sim 3$, for the NLR derived from the Balmer decrement (Koski 1978) predicts X-ray absorption of at least $N_{\text{H}} = 6 \times 10^{21} \text{ cm}^{-2}$ on the scattered continuum, if the standard gas-to-dust ratio is assumed (and the gas is not ionized). Since there is no evidence for such large absorption in the spectrum, the soft X-ray emission is likely to originate from the region outside the nucleus, where presumably a starburst is taking

Table 5. Results of spectral fits to the ASCA data of Mrk273. The 0.5–10 keV SIS data and the 1–10 keV GIS data are fitted jointly. The value of χ^2 for this fit is 110.4 for 129 degrees of freedom. A and A_{PL} are normalizations of the MEKAL and power-law (PL) models at 1 keV in unit of ${}^*10^{-14}(4\pi D^2)^{-1} \int dV$, and $\dagger \text{ph keV}^{-1} \text{s}^{-1} \text{cm}^{-2}$, respectively. The PL₁ can be replaced by a thermal emission model with a temperature of ~ 5 keV, without significant difference in statistics. The EW of the line is ~ 520 eV.

	kT keV	Z Z_{\odot}	A *	N_{H} cm^{-2}
MEKAL	$0.47^{+0.24}_{-0.15}$	$0.23(> 0.03)$	8.9×10^{-5}	1.1×10^{20}
		Γ	A_{PL} \dagger	N_{H} cm^{-2}
PL ₁	$1.7^{+1.0}_{-0.6}$		6.4×10^{-5}	$1^{+1}_{-1} \times 10^{21}$
PL ₂	1.8		5.2×10^{-4}	$4.3^{+1.2}_{-1.3} \times 10^{23}$
		E_{line} keV		I_{line} $\text{ph s}^{-1} \text{cm}^{-2}$
Gaussian		$6.39^{+0.22}_{-0.20}$		$1.0^{+0.9}_{-0.5} \times 10^{-5}$

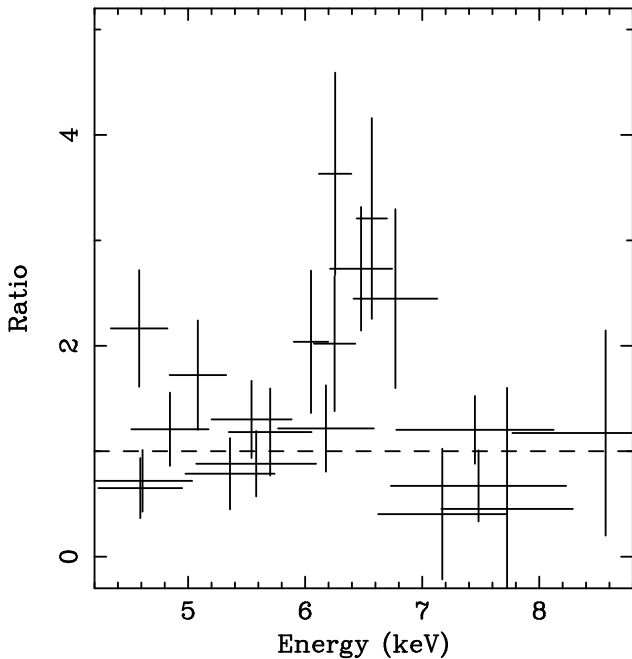


Figure 3. The iron K line feature of Mrk273. The ratio of the ASCA data and the best-fit absorbed power-law continuum is plotted. The energy scale is corrected for the redshift ($z = 0.038$). This feature is consistent with a single narrow-line at 6.4 keV.

place. Results of the two-component fits to the soft X-ray data are shown in Table 5. Here the Galactic absorption by $N_{\text{H}} = 1.1 \times 10^{20} \text{ cm}^{-2}$ is assumed for the low temperature thermal spectrum. Whether the power-law or high temperature ($kT \geq 5$ keV) thermal spectrum to be added to the $kT = 0.45$ keV thermal model is difficult to distinguish at the present quality of data.

Excess emission is seen above 3 keV as well as an iron K line at ~ 6.4 keV (Fig. 3). The 3–10 keV continuum is very flat ($\Gamma = 0.1 \pm 0.4$). The flat spectrum is probably due to absorption of which the spectral cut-off is masked by the soft X-ray component emitted outside the X-ray absorbing material. If a power-law of $\Gamma = 1.8$ is assumed for the spec-

trum of the absorbed source, the absorption column density is $N_{\text{H}} \simeq 4 \times 10^{23} \text{ cm}^{-2}$. An extrapolation of the power-law is well below the upper limit given by the CGRO/OSSE observation (Dermer et al 1997). The 2–10 keV luminosity corrected for the absorption is $5 \times 10^{42} \text{ erg s}^{-1}$. The iron K line feature is consistent with a single, narrow 6.4 keV line and there is no strong evidence for higher energy lines (see Fig. 3). The EW of the line is about 520^{+470}_{-260} eV.

An alternative model for the flat hard X-ray spectrum is reflection from cold material. A very large EW of iron line (e.g., $EW \geq 1$ keV) is often observed in the reflection spectrum. The reflection-dominated spectrum has a very hard continuum above 10 keV and would have the 20–100 keV flux of $\sim 4 \times 10^{-12} \text{ erg cm}^{-2} \text{ s}^{-1}$ (estimated assuming a pure reflection case of the XSPEC model, `pexrav`, Magdziarz & Zdziarski 1995), which is still consistent with the OSSE upper limit.

4.3 Arp220

The double nucleus in Arp220 is clearly seen in near-IR images (Graham et al 1990; Scoville et al 1998). The large far-IR excess in the energy distribution makes this galaxy one of the most luminous sources in the nearby universe within 100 Mpc. The nuclear region shows a signature of high excitation gas ($[\text{OIII}]\lambda 5007/\text{H}\beta \sim 10$, Sanders et al 1988) while the emission-line nebula shows LINER characteristics at larger radii (Heckman et al 1990). This galaxy is a famous example of the ionization photon deficit problem (DePoy et al 1987; Leitherer & Heckman 1995), which casts a doubt on the starburst interpretation for the major energy source in this galaxy despite the lack of direct evidence for an AGN.

4.3.1 The ASCA images and spectrum

As the ROSAT PSPC image (observed between 1993 July 24 and August 3, Heckman et al 1996) shows, another extended X-ray source is observed to the south of Arp220 (“the southern source”). Heckman et al (1996) associate the source with

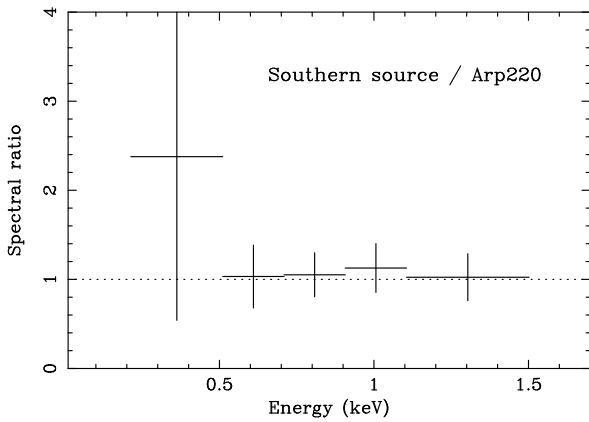


Figure 4. Plot of spectral ratio of the southern source and Arp220 made from the ROSAT PSPC data. The southern source appears to have a similar spectrum and flux to Arp220 in the ASCA band (≥ 0.5 keV).

a distant ($z \sim 0.1$) group of galaxies or a poor cluster. Optical spectroscopy of galaxies at the extended X-ray source shows that those galaxies are at redshift of 0.08 (J. Hibbard, private communication) which supports the group/cluster interpretation. No matter whether it is physically associated with Arp220, both sources have similar soft X-ray spectra and fluxes (Fig 4; also see Table 1 in Heckman et al 1996). Arp220 and the southern source are resolved also in the ASCA SIS 0.5–2 keV image (Fig 5a). However, in the energy band above 2 keV, no significant X-rays are detected from the south source but only Arp220 (Fig. 5b). As the energy spectrum shows (Fig 6), no X-ray emission is detected above 5 keV even in the GIS image.

An image analysis estimates about half (~ 46 per cent) of the 0.5–2 keV observed counts is attributed to Arp220, hence half the observed flux because of similar spectral shapes of the two sources in the energy band (the Einstein IPC flux, e.g., David, Jones & Forman 1992, was overestimated by a factor of ~ 2). At the spectral resolution of the SIS, an emission line peak due to Fe L around 0.8–0.9 keV is evident, implying thermal emission. There is also a faint hard X-ray component up to 5 keV.

The ASCA spectrum (Fig. 6) is modelled in a similar way to that for Mrk231. Spectral fitting results are summarized in Table 4. The X-rays from the ‘southern source’ are contained in the ASCA spectrum. Observed fluxes in the 0.5–2 keV and 2–10 keV bands are 1.7×10^{-13} erg cm $^{-2}$ s $^{-1}$ and 2.2×10^{-13} erg cm $^{-2}$ s $^{-1}$, respectively. The characteristic temperature of the extended thermal emission is $kT = 0.76^{+0.13}_{-0.11}$ keV and the metallicity is $0.3 (\geq 0.1) Z_{\odot}$. This component has a 0.5–2 keV luminosity of 8.4×10^{40} erg s $^{-1}$ at the distance of Arp220 of which $\sim 3.9 \times 10^{40}$ erg s $^{-1}$ comes from Arp220. The hard component modelled by an absorbed power-law with a photon-index of 1.8 requires absorption by $N_{\mathrm{H}} = 6^{+12}_{-6} \times 10^{21}$ cm $^{-2}$. A photon index ranging between 1.2 and 4.8 is allowed for the power-law. If a thermal emission model replaces the power-law, its temperature would be about 2 keV but with large

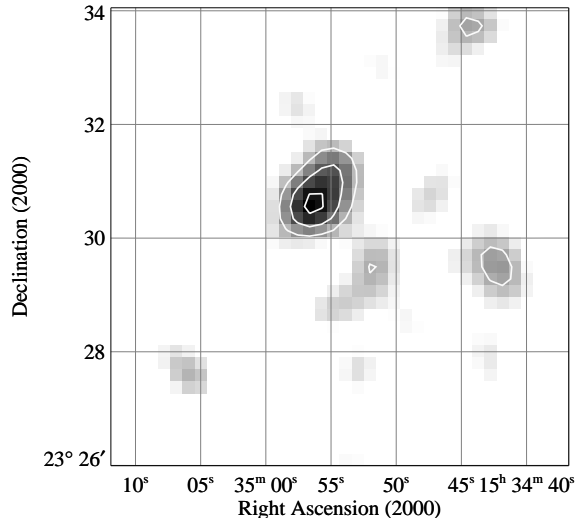
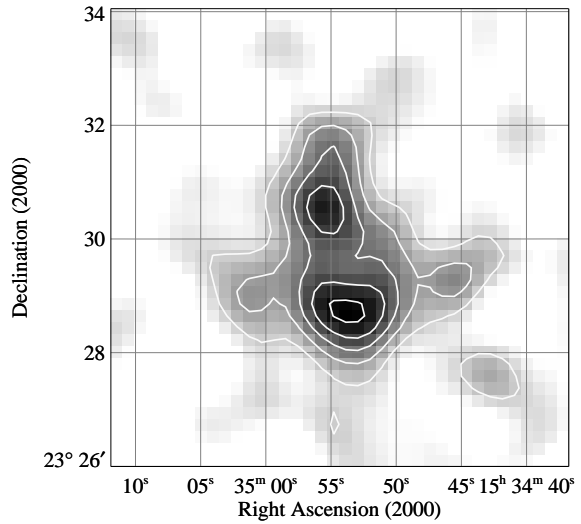


Figure 5. The ASCA SIS images of Arp220 region obtained in the energy bands of 0.5–2 keV (upper panel) and 2–5 keV (lower panel). Arp220 and the southern source are resolved in the soft band image whilst only Arp220 is detected in the hard band image.

uncertainties. The lack of significant X-ray detection at the iron K band means no useful constraint available for an iron line strength. The 2–10 keV flux of this hard component is 2.1×10^{-13} erg cm $^{-2}$ s $^{-1}$ and a corresponding absorption-corrected luminosity is 1.4×10^{41} erg s $^{-1}$.

4.4 NGC6240

Many properties of NGC6240 have been interpreted in terms of intensive star formation (e.g., Majewski et al 1993; Ridgway et al 1994; Shier, Rieke & Rieke 1996). The near-IR spectrum is well accounted for by a starburst stellar population. Extremely strong molecular hydrogen lines, e.g., H₂

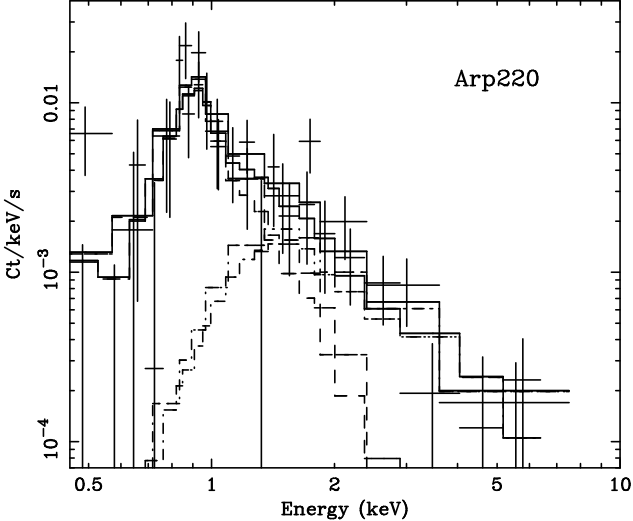


Figure 6. The ASCA SIS spectrum of Arp220. The data are fitted with a model consisting of a thermal emission spectrum and an absorbed power-law. Note that the data are a sum of Arp220 and the southern source which contributes a half of the total flux below 2 keV with a similar spectral shape to that of Arp220.

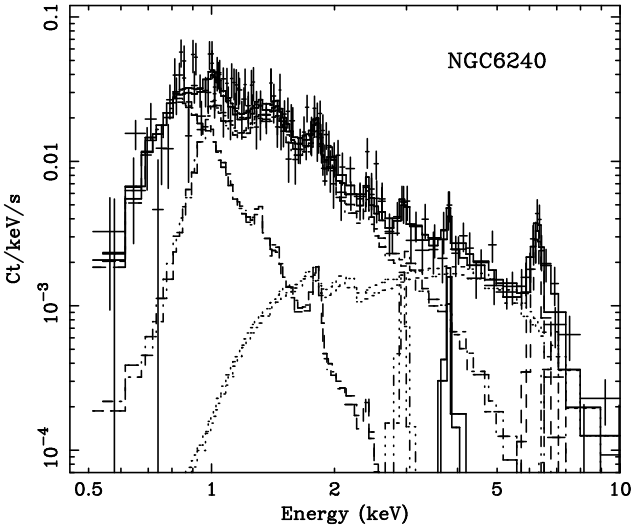


Figure 7. The ASCA SIS spectrum of NGC6240. The data are fitted with a model consisting of a two-temperature thermal emission spectrum and an absorbed power-law with emission-lines due to Ar, Ca, and Fe K α . Detailed spectral analysis is described in Iwasawa & Comastri (1998).

S(1) at $2.1\mu\text{m}$, have been noticed (DePoy et al 1986; van der Werf et al 1993; Ridgway et al 1994). The LINER-like optical spectrum and the large velocity field ($\sim 1000 \text{ km s}^{-1}$) in the nuclear region can be explained as results from an outflow driven by a starburst (Heckman et al 1990). The extended H α nebula is $\sim 50 \times 60 \text{ kpc}$ in size and $\sim 10^{42} \text{ erg s}^{-1}$ in luminosity, which is larger and more powerful than Arp220 despite the smaller infrared luminosity. Luminous extended soft X-ray emission ($\sim 10^{42} \text{ erg s}^{-1}$) has also been found with the ROSAT PSPC (Schulz et al 1998; Iwasawa & Comastri 1998) and HRI (Komossa et al 1998). NGC6240 is

the brightest X-ray source among the four FIRGs presented here.

The ASCA results on NGC6240 have been published by several authors (Kii et al 1997; Turner et al 1997). A detailed spectral analysis is reported in Iwasawa & Comastri (1998). Schultz et al (1998) and Netzer, Turner & Gerge (1998) attribute 80 per cent and all the soft X-ray emission to scattered AGN light, based on the ROSAT PSPC data and the ASCA data, respectively. However, the ASCA soft X-ray spectrum is modelled by two-temperature thermal emission in Iwasawa & Comastri (1998), who interpret it as absorbed high-temperature gas and low-temperature, spatially more extended gas produced by a starburst (see Fig 7). Since the HRI image shows that a large fraction (> 70 per cent) of the 0.1–2.4 keV flux is extended outside the PSF of the HRI ($\sim 2.4 \text{ kpc}$ in radius at NGC6240), we are in favour of the starburst interpretation for the soft X-ray emission. The central bright part of the soft X-ray nebula is nearly spherical and has a size of about 10–20 kpc across (see Komossa et al 1998), which may be related to the bright hourglass-shaped region ($10 \times 7 \text{ kpc}$) of the H α nebula imaged by Heckman et al (1987).

The ASCA spectrum above 3 keV is very flat and shows a prominent iron K line feature around 6.5 keV. The most likely interpretation of these spectral signatures in the hard X-ray band is reflection of a buried AGN radiation, predominantly from cold, thick material. The lack of detection of an absorbed component up to 10 keV implies that the column density of the matter occulting any central strong X-ray source exceeds $\sim 2 \times 10^{24} \text{ cm}^{-2}$. The similarity of the ASCA spectrum above 3 keV to NGC1068 (Ueno et al 1994; Iwasawa et al 1997) renders an analogous argument on the luminosity of a central source possible, given a likely estimate of the central source of NGC6240 ($\sim 10^{44} \text{ erg s}^{-1}$, Pier et al 1994). The 3–10 keV luminosity of NGC6240, $2 \times 10^{42} \text{ erg s}^{-1}$, an order of magnitude above that of NGC1068, suggests that the FIRG may contain a QSO nucleus emitting at $\sim 10^{45} \text{ erg s}^{-1}$.

5 COMPOSITE X-RAY SPECTRUM

5.1 Thermal and nonthermal X-ray emission

The X-ray spectra of FIRGs consists of multiple components in the 0.5–10 keV band. Thermal emission features are seen in the soft X-ray band. Some fraction of observed soft X-ray emission may be due to the scattered light of a hidden AGN (e.g., Mrk273). However, as the ROSAT HRI images of Arp220 (Heckman et al 1996) and NGC6240 (Komossa et al 1998) show, most of the soft X-ray emission is extended, implying that thermal emission produced by a starburst is the likely source. On the other hand, the hard X-ray spectrum is an important probe for AGN. Particularly, the presence of a strong 6.4 keV line from Fe K α is a crucial diagnostic of obscured AGNs (Mrk273 and NGC6240). The spectral shape and intensity of hard X-ray emission strongly depends on the absorption column density: the energy of the absorption cut-off is a function of N_{H} , and when N_{H} exceeds $\sim 2 \times 10^{24} \text{ cm}^{-2}$, the absorbed direct emission from a central source would disappear beyond the ASCA band-pass ($> 10 \text{ keV}$) and leave the ASCA hard band spectrum dominated by weak reflected light (NGC6240).

To characterize the X-ray spectra of the FIRGs, it is useful to compare with X-ray spectra showing characteristic features of each component observed in well-known starburst and Seyfert-2 galaxies. We selected a typical sample of starburst (M82), Compton-thick Seyfert 2 (NGC1068 and NGC4945), and Compton-thin Seyfert 2 (NGC4507 and NGC4388) galaxies. All the ASCA SIS spectra are shown in Fig. 8 as well as the sample FIRGs. Note that the data for Arp220 have been corrected for the contribution from ‘the southern source’.

5.2 Comparison sample

5.2.1 M82

M82 is a nearby ($D = 3$ Mpc) well-studied starburst galaxy. This galaxy shares many properties with the FIRGs presented in this paper but less powerful in terms of infrared luminosity ($3 \times 10^{10} L_\odot$). Extended soft X-ray emission has been detected with the Einstein Observatory (Fabbiano 1988). The large soft X-ray nebula extends along the superwind structure, i.e., the minor axis of the edge-on galaxy disk.

The ASCA spectrum of M82 has been studied by several authors (Moran & Lehnert 1997; Ptak et al 1997; Tsuru et al 1997). Its multi-temperature nature has been known from spectral analysis (see Tsuru et al 1997). There is significant hard X-ray emission above 3 keV ($\sim 2 \times 10^{40} \text{ erg s}^{-1}$), but the iron K feature is very faint. Although the origin of the hard X-ray emission is not entirely understood, the presence of ArXVII(3.1 keV) and CaXIX(3.9 keV) suggests that a significant fraction is of thermal origin. The BeppoSAX data rule out a power-law spectrum (M. Cappi, private com.). The significant detection of a Fe K line at 6.7 keV in the BeppoSAX spectrum of a similar starburst galaxy NGC253 strongly supports the thermal emission interpretation (Mariani et al 1998).

The observed 0.5–10 keV luminosity is $3.2 \times 10^{40} \text{ erg s}^{-1}$. Extended soft X-ray emission has been resolved with the ASCA SIS because of the proximity of the galaxy. It has been found that that the X-ray spectrum is softer in the outer region than in the central region.

5.2.2 NGC1068

NGC1068 is a classical Compton-thick Seyfert 2 galaxy ($D = 14.4$ Mpc). Since the discovery of polarized broad-line emission by Antonucci & Miller (1985) this galaxy provides the strongest case for the unification scheme of both types of Seyfert galaxies. NGC1068 is also a powerful infrared source ($2 \times 10^{11} L_\odot$, Telesco et al 1984). In the circumnuclear region, a dense molecular disk of a 100 pc scale (Jackson et al 1993; Tacconi et al 1994) and kilo parsec scale star forming arms (Helfer & Blitz 1995) have been found. A clear difference from the FIRGs is its clear view to the Seyfert 2 nucleus, i.e., the NLR. The reddening to the NLR is small ($A_V \sim 0.2$).

In X-rays, the detection of a strong Fe K line with Ginga (Koyama et al 1989) made this object the first example of Compton-thick Seyfert 2s. No detection of an absorbed X-ray source up to 100 keV means that the line-of-sight column density should be far above 10^{25} cm^{-2} (Matt et al 1997). A sub-parsec scale, nearly edge-on (inclination of larger than

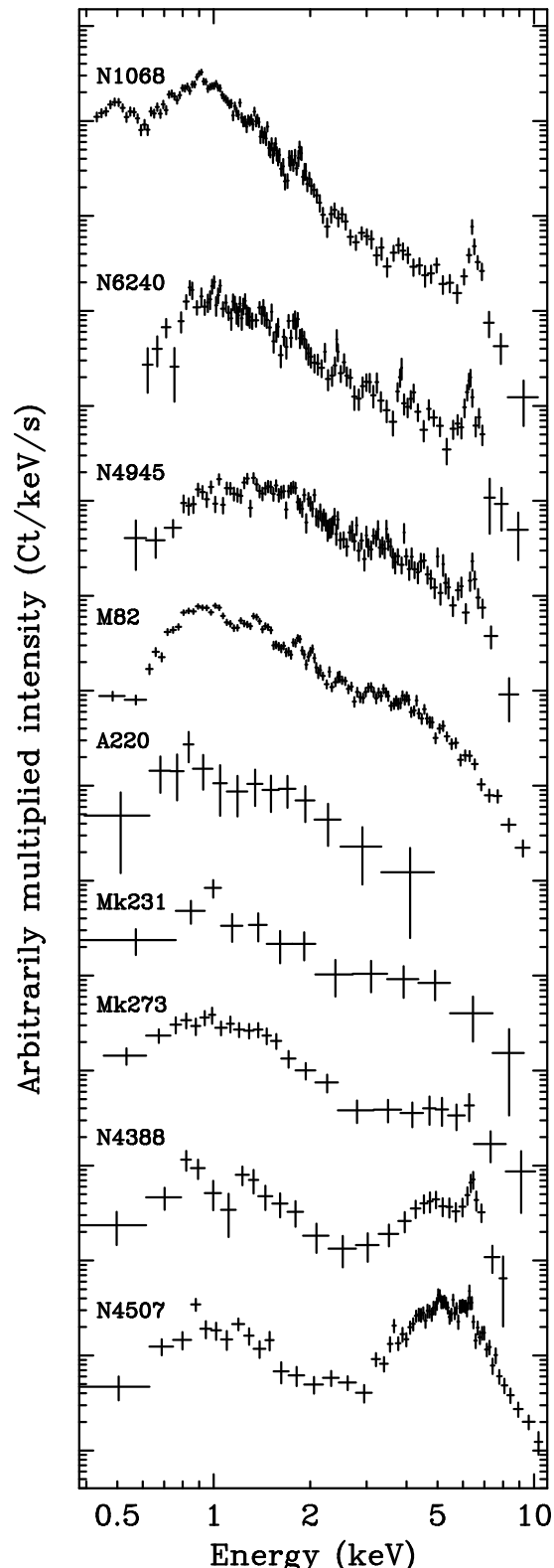


Figure 8. The ASCA SIS spectra of NGC1068, NGC6240, NGC4945, M82, Arp220, Mrk231, Mrk273, NGC4388 and NGC4507 (from up to bottom). The y-axis is in unit of counts $\text{keV}^{-1} \text{s}^{-1}$ but arbitrarily multiplied for clarity. The Arp220 spectrum has been corrected for the contamination from ‘the southern source’. See details for individual objects in Section 5.2 and for comparisons in Section 5.3.

Table 6. Ratios of the ROSAT PSPC count rate between the hard (0.5–2 keV) and the full (0.1–2 keV) bands. The count rates are corrected for background.

	Mrk231	Mrk273	Arp220	NGC6240
0.5–2/0.1–2 keV	0.62 ± 0.06	0.73 ± 0.09	0.92 ± 0.14	0.93 ± 0.11

80°) disk has been discovered by high-resolution radio imageries in H_2O maser and continuum (Greenhill et al 1996; Gal-limore et al 1997), which presumably hides a central X-ray source.

The soft X-ray emission is spatially extended (Wilson et al 1992) and almost certainly associated with starburst activity in the circumnuclear region. The soft X-ray portion of ASCA spectrum (≤ 3 keV) is dominated by thermal emission described by a two-temperature model (Ueno et al 1994). The X-ray properties of NGC1068 is reviewed by Wilson & Elvis (1997). As shown in Fig. 8, the X-ray spectrum shows an enormous excess in soft X-ray.

5.2.3 NGC4945

NGC4945 is a nearby ($D = 3.9$ Mpc) FIRGs containing a *nearly* Compton-thick nucleus. This galaxy is a far-IR excess galaxy with similar properties and luminosity to M82. The nucleus is heavily reddened and there is little evidence for an active nucleus apart from hard X-ray band. Superwind features, e.g., a hollow-cone shaped optical image (Nakai 1989), split optical emission line profiles (Heckman et al 1990), have been found. The optical emission-line gas in the nuclear region shows LINER type excitation (Whiteoak & Gardner 1978).

A variable hard X-ray (10–30 keV) source was identified with this galaxy using Ginga observations, which is heavily absorbed by a column density of $\sim 5 \times 10^{24} \text{ cm}^{-2}$ thus only visible above 10 keV (Iwasawa et al 1993). The detection of bright hard X-ray emission (~ 100 keV) by the CGRO/OSSE confirmed it (Done et al 1996). The absorption-corrected 2–10 keV luminosity is estimated to be $2 \times 10^{41} \text{ erg s}^{-1}$. Bright H_2O maser emission ($\sim 57L_\odot$) has been found (Dos Santos & Lepine 1979; Baan 1985; Braatz, Wilson & Henkel 1996; Greenhill, Moran & Her-rinstein 1997). Like NGC1068, the water maser disk can be roughly approximated to a Keplerian disk on parsec scale (Greenhill et al 1997).

A strong Fe K complex and reflection continuum are observed at the nuclear position of the galaxy and an extended X-ray nebula with some point sources (e.g., Iwasawa 1995; Brandt, Iwasawa & Reynolds 1996) are also resolved. Therefore, the X-ray emission observed with ASCA consists both of the reflected AGN emission and starburst emission. Since the bandpass of ASCA is limited to energies below 10 keV, the absorbed component is invisible. The absorption in the soft X-ray band (< 1 keV) is mainly due to the large Galactic extinction ($N_{\text{H}} \sim 1.5 \times 10^{21} \text{ cm}^{-2}$, Dickey & Lockman 1990) because of the low Galactic latitude ($b \sim 15^\circ$).

5.2.4 NGC4388 and NGC4507

These two Seyfert 2 galaxies contain typical Compton-thin sources absorbed by $N_{\text{H}} \approx (4-5) \times 10^{23} \text{ cm}^{-2}$. In the ASCA

band, the the direct radiation from the central source is still visible above the absorption cut-off at 4–5 keV. With this amount of absorption, a strong hard X-ray excess is seen, often associated with a 6.4 keV Fe K line. The heavily absorbed hard X-ray component is more prominent in NGC4507 than NGC4388. The ASCA results have been reported by Iwasawa et al (1997) for NGC4388 and Comastri et al (1997) for NGC4507. The estimated 2–10 keV luminosities corrected for the absorption are $2 \times 10^{42} \text{ erg s}^{-1}$ for NGC4388 and $2 \times 10^{43} \text{ erg s}^{-1}$ for NGC4507.

The weak soft X-ray emission is mainly due to the scattered light in NGC4507 (Comastri et al 1997) while a significant fraction of the soft X-rays observed below 2 keV in NGC4388 orginates in the extended thermal emission resolved with the ROSAT HRI (Matt et al 1994).

5.3 The X-ray spectra of the FIRGs and the comparison sample

In Fig. 8, almost entire or a significant fraction of soft X-ray emission is due to thermal emission originating from starbursts in all galaxies except for NGC4507. Note that the exceptionally large soft X-ray excess emission in NGC1068 compared with the other galaxies, which may be related to absorption in the starburst regions, as discussed in Section 6.1.2. The spectrum of M82 is presumably of a typical starburst without any significant AGN component. A clear difference from the other Seyfert 2 spectra is the absence of a strong Fe K line.

The two Compton-thick Seyfert 2s (NGC1068 and NGC4945) show very strong Fe K features ($EW > 1$ keV), indicative of reflection-dominated spectrum. The detection of a similar Fe K feature in NGC6240 has revealed a Compton-thick source in the FIRG despite the rest of the ASCA spectrum resembling M82.

The two Compton-thin Seyfert 2 galaxies (NGC4388 and NGC4507) show clear hard X-ray excess due to strong absorption. The 6.4 keV Fe K lines with EW of few hundreds eV are also seen. Mrk273 is most likely classified as this type but its hard X-ray excess is less prominent. The relatively flat 3–10 keV spectrum suggests that Mrk231 is also the case. As shown in the spectral analysis (Section 4.1.2 and Fig. 1) the absorption would be smaller (few times of 10^{22} cm^{-2}) than the other three objects. However, the origin of the hard X-ray emission is not yet clear from the present data and several possibilities are discussed in Section 6.2.2. For the Compton-thin sources, sources with a stronger hard X-ray excess are placed lower in Fig. 8.

Arp220 lacks hard X-ray emission above 5 keV and the ASCA spectrum appears to be softer than the other objects, although the signal to noise ratio of the data is poor.

5.4 The ROSAT band colour

The ROSAT bandpass extends down to 0.1 keV, which is more sensitive to the low temperature thermal emission than ASCA. The hardness ratio obtained from the ROSAT PSPC data for the four FIRGs are shown in Table 6, to assess their soft X-ray band (0.1–0.5 keV) spectra.

Arp220 and NGC6240 have harder spectra than those of Mrk231 and Mrk273 in the ROSAT band. It is uncertain whether the hardness is due to a higher averaged temperature or larger absorption.

6 DISCUSSION

6.1 Starburst properties

6.1.1 X-ray luminosities

Based on the spectral analysis of the ASCA data, we assume that the observed soft X-ray emission below 2 keV is predominantly thermal emission originating from a starburst in those galaxies. Then we compare the soft X-ray luminosities with the other possible indicators of a starburst. We note that it is premature to claim any correlation from these comparisons because of the small size of the sample, and the trends seen here must be tested by a larger sample.

Far-IR luminosity is generally thought to be a good indicator of starburst intensity. However, Arp220 is far more powerful in the far-IR, relative to other bands, e.g., the soft X-ray emission (Fig. 9), H α , optical light (L_B , see Table 1), than the other FIRGs. The far-IR excess in Arp220 is discussed in Section 6.3

Conceivably, starburst-driven galactic outflow is a main heating source of the extended optical emission-line nebulae (Heckman et al 1990). Armus et al (1990) show that more than half of the total H α +[NII] luminosity (not corrected for internal reddening) comes from outside the central 2×2 kpc box and the sizes of the nebulae are a few tens kpc in the FIRGs apart from Mrk231, in which the broad H α line observed in the nucleus dominates the total luminosity. Shock heating of the ISM by the outflow is also a likely source of the soft X-ray emission, as supported by the soft X-ray morphology aligned with a superwind structure in nearby starburst galaxies like M82 (e.g., Fabbiano 1988; Strickland et al 1997). In fact, the luminosity ratio of the H α +[NII] and soft X-ray (0.5–2 keV) of the FIRGs are similar to each other (2.6–5.5; Fig. 10) while M82 has a larger value (~ 13).

On the other hand, a starburst stellar population appears to account for the near-IR emission in the FIRGs except for Mrk231 (Ridgway et al 1994; Shier et al 1996). A correlation between the $2.2\mu\text{m}$ and the soft X-ray luminosity is relatively good (Fig. 11). The excess of the $2.2\mu\text{m}$ emission in Mrk231 is probably due to a contribution from the AGN, as suggested from the near-IR properties (Fig. 12; blue $H - K$ colour and the very shallow CO absorption feature at $2.3\mu\text{m}$). It should be noted that optical depths at $2.2\mu\text{m}$ and the soft X-ray band are similar to each other if the standard gas-to-dust ratio is assumed.

In summary, the soft X-ray emission, extended optical emission-line nebulae, and near-IR emission are consistent with each other in the context of starburst, but not with the far-IR emission.

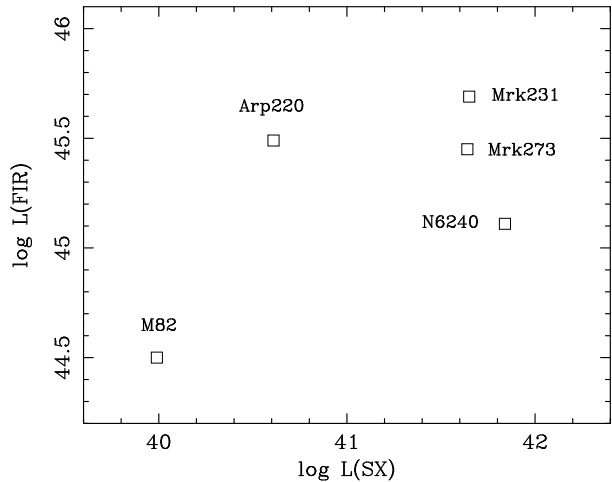


Figure 9. Plot of the far-IR luminosity against the 0.5–2 keV (SX) luminosity (Table 7). Note the large excess in the far-IR of Arp220.

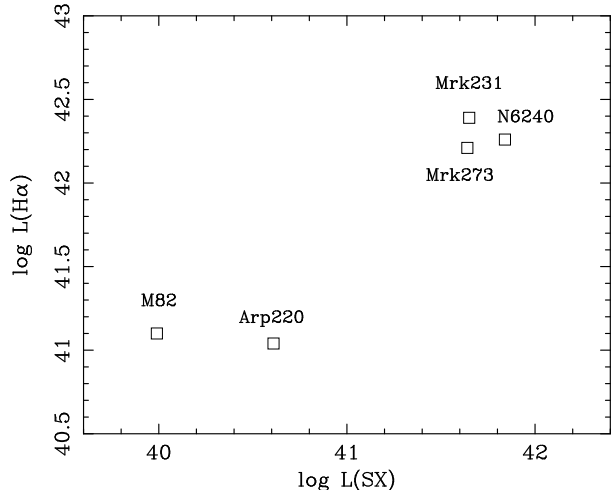


Figure 10. Plot of the total H α +[NII] luminosity against the 0.5–2 keV (SX) luminosity (Table 7).

6.1.2 Temperature and absorption structure in the X-ray nebulae

At the low quality of the present data, a single temperature model is a sufficient description for the starburst soft X-ray emission. However, some good quality data like of M82 (Tsuru et al 1997; Strickland et al 1997) and NGC6240 (Iwasa & Comastri 1998) have provided evidence for multi-temperature gas and absorption for the starburst regions. Obscured, hot gas in the near-nuclear region and cooler gas at larger radii are expected from the superwind scenario (Chevarier & Clegg 1985; Tomisaka & Ikeuchi 1988). High obscuration in starburst nuclei have also been inferred from optical and infrared observations of starburst (e.g., M82, Heckman et al 1990) and ultraluminous infrared galaxies (Roche et al 1983; Thronson et al 1990; Lutz et al 1996; Dudley & Wynn-Williams 1997).

The size of the starburst region in far-IR galaxies appears to be compact (dense molecular disk in Mrk231 and Arp220 are inferred to be few hundreds pc in radius, Bryant

Table 7. Far-infrared, $2.2\mu\text{m}$, optical emission-line ($\text{H}\alpha + [\text{NII}]$), and X-ray luminosities (erg s^{-1}) of the FIRGs and M82. $L(\text{FIR})$ and $L(\text{H}\alpha)$ are taken from Armus, Heckman & Miley 1990. Note that values listed in Lonsdale et al (1985) are used for $L(\text{FIR})$. The $2.2\mu\text{m}$ power is calculated using the measurements by Ridgway et al (1994). The $L(\text{H}\alpha)$ is total luminosity for the extended emission line nebula (no correction for reddening). $L(\text{SX})$ and $L(\text{HX})$ are observed X-ray luminosities in the 0.5–2 keV and 2–10 keV bands, respectively (no correction for absorption).

Galaxy	$\log L(\text{FIR})$ erg s^{-1}	$\log P(2.2\mu\text{m})$ $\text{erg s}^{-1}\mu\text{m}^{-1}$	$\log L(\text{H}\alpha)$ erg s^{-1}	$\log L(\text{SX})$ erg s^{-1}	$\log L(\text{HX})$ erg s^{-1}
Mrk231	45.69	45.20	42.39	41.65	42.32
Mrk273	45.45	44.23	42.21	41.64	42.19
Arp220	45.49	43.52	41.04	40.61	41.06
NGC6240	45.11	44.38	42.26	41.84	42.35
M82	44.50	42.15	41.10	39.99	40.35

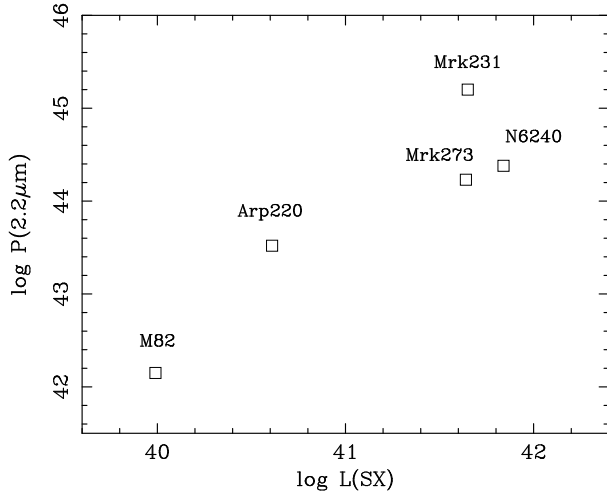


Figure 11. Plot of $2.2\mu\text{m}$ power ($\text{erg s}^{-1}\mu\text{m}^{-1}$) against the 0.5–2 keV (SX) luminosity (Table 7).

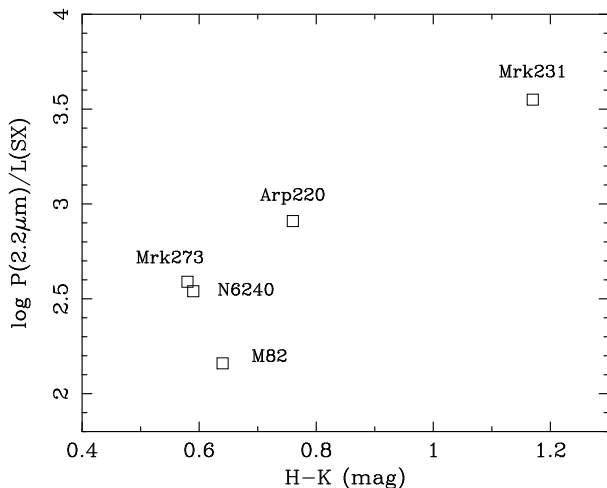


Figure 12. Plot of the luminosity ratio between $2.2\mu\text{m}$ and the soft X-ray (0.5–2 keV) emission against the near-IR colour ($H - K$). The values of $H - K$ are taken from Ridgway et al (1994) and references therein.

& Scoville 1996; Scoville et al 1997). A compact starburst near the nucleus has also been found in some Seyfert 2 galaxies (e.g., Mrk477, Heckman et al 1997). In contrast, the starburst ring in NGC1068 is on rather large scale (few kpc) and well separated from the Seyfert 2 nucleus (Neff et al 1994). The compact starburst regions are likely to be more obscured than the large scale starburst region in NGC1068. The much softer spectrum of NGC1068 in the low energy X-ray band than the other FIRGs (Fig. 8) is therefore suspected to be due to the difference of obscuration. The correction for absorption would be important for estimating the true starburst luminosity through X-ray data. High quality data from future observations are required to decompose the gas structure.

6.2 AGN properties (Mrk273, NGC6240 and Mrk231)

6.2.1 Mrk273 and NGC6240

The absorption-corrected 2–10 keV luminosity of Mrk273 is only $5 \times 10^{42} \text{ erg s}^{-1}$, nearly three orders of magnitude below the far-IR luminosity. This suggests that Mrk273 contains an obscured AGN which is not a QSO nucleus which would provide the bulk of the bolometric luminosity, but a moderate-luminosity Seyfert. However, note that since a reflection-dominated spectrum is not ruled out by the present data (see Section 4.2.2), the intrinsic luminosity of the hidden AGN could be as high as QSOs.

The heavily obscured X-ray nucleus in the nearby Seyfert 2 galaxy NGC4945 has the 2–10 keV luminosity of $\sim 10^{41} \text{ erg s}^{-1}$ after correction for absorption. It is also three orders of magnitude below the far-IR luminosity. In these cases, the obscured AGN do not play a major role in powering the far-IR emission and starbursts are probably the most important energy source. In fact, the mid-IR properties of NGC4945 are in excellent agreement with those of the other starburst galaxies (Genzel et al 1998). The lack of AGN features in the mid-IR band can easily be understood, considering the extremely thick obscuration of the central source in NGC4945 implied from X-ray observations ($N_{\text{H}} \simeq 5 \times 10^{24} \text{ cm}^{-2}$, or $\tau_{30\mu\text{m}} \sim 25$, Iwasawa et al 1993; Done et al 1996). The detection of high excitation mid-IR lines, e.g., [OIV] $26\mu\text{m}$, [NeV] $14.3, 24.3\mu\text{m}$, in Mrk273 from the ISO/SWS (Genzel et al 1998) is probably due to the smaller obscuration of the central source ($N_{\text{H}} \sim 5 \times 10^{23} \text{ cm}^{-2}$, $\tau_{30\mu\text{m}} \sim 2$). Alternatively, perhaps the

X-ray source has now faded to its low state, leaving the large EW (~ 500 eV) of the Fe K line from a distant line emitter as a reverberation effect (e.g., Mrk3, Iwasawa et al 1994; NGC2992, Weaver et al 1996).

NGC6240 is suspected of harbouring a QSO nucleus, possibly emitting at 10^{45} erg s $^{-1}$. The estimated QSO luminosity, almost comparable with the far-IR luminosity, suggests that the hidden QSO makes a significant contribution to the far-IR (bolometric) luminosity and may even dominate it. The galaxy is the most powerful soft X-ray emitter among the four FIRGs presented here, indicating that the starburst is also powerful. Having both powerful an AGN and a starburst as energy sources, despite the small far-IR luminosity (Table 7) compared to the other FIRGs may be a problem. If the superwind heating the soft X-ray/H α nebula is mainly driven by a QSO instead of starburst, this problem could be relaxed.

The estimate of the intrinsic AGN luminosity in NGC6240 relies on the bolometric (optical to X-ray) luminosity of a hidden Seyfert 1 nucleus in NGC1068 (3×10^{44} (14 Mpc/ D) 2 (0.01/ f_{refl}) $^{-1}$ erg s $^{-1}$, where D is the distance to NGC1068 and f_{refl} is the fraction of light from the hidden nucleus reflected into our line of sight) given by Pier et al (1994). The validity of their estimate is justified by the fact that they used polarization measurements, which are expected to be affected little by possible stellar light contamination, otherwise the derived intrinsic luminosity of NGC1068 (and thus NGC6240) would be overestimated.

The central source of NGC6240 should be occulted by thick material with a column density over 2×10^{24} cm $^{-2}$ along the line of sight. Since no strong evidence for an AGN has been found in this galaxy, apart from the hard X-ray spectrum, the powerful starburst masks the AGN phenomenon in a more heavily-obsured region inside.

6.2.2 Mrk231

Although the X-ray emission with the hard spectrum above 3 keV may be attributed to an AGN, the observed X-ray luminosity is quite small ($L_{2-10\text{keV}} \sim 2 \times 10^{42}$ erg s $^{-1}$), compared to the infrared luminosity and the reddening-corrected optical luminosity ($M_V \sim -25.1$, Boksenberg et al 1977), both of which are in the range of QSOs.

The nucleus of Mrk231 clearly shows manifestations of a Seyfert-1 or BAL QSO type active nucleus in various wavebands. The broad (FWHM ~ 4200 km s $^{-1}$) H α was measured at luminosity of 7×10^{42} erg s $^{-1}$ by Boksenberg et al (1977), while Armus et al (1990) measured 2×10^{42} erg s $^{-1}$ within the central 2×2 kpc region. The observed small X-ray luminosity is difficult to understand as a normal Seyfert 1 or QSO. The good correlation between 2–10 keV and H α luminosity ($\log[L(2-10\text{keV})/L(H\alpha)] \sim 1$) found in Seyfert 1 galaxies and QSOs (Ward et al 1988) predicts that the 2–10 keV luminosity of Mrk231 would be $(2-7) \times 10^{43}$ erg s $^{-1}$, which is at least 10 times higher than the observed value.

The difference between the two H α measurements could be due to variability of the line, and may suggest a declining central source. An inspection of the X-ray data from earlier mission like HEAO-1 however suggests that the past activity in the hard X-ray band was also weak (2×10^{-11} erg cm $^{-2}$ s $^{-1}$; the X-ray flux expected from the (2–10keV)–H α correlation and the Boksenberg et al (1977)

measurement is below the flux limit (3.1×10^{-11} erg cm $^{-2}$ s $^{-1}$ from the HEAO-1 A2 survey by Piccinotti et al 1982; Rieke 1988 gave an upper limit of 6.5×10^{-12} erg cm $^{-2}$ s $^{-1}$ based on the HEAO-1 A1 survey). Possible explanations for the X-ray quietness are discussed below.

(i) A powerful starburst (absence of AGN)

The hard X-ray component may be attributed to high temperature gas produced by a starburst. A powerful starburst which is two orders of magnitude more luminous than M82 is required if simply scaled. The lack of detection of of high excitation lines in the ISO/SWS mid-IR spectrum of Mrk231 and inferred large reddening (Rigopoulou et al 1998) may support this hypothesis. However, many properties, not usually seen in starburst galaxies but in AGNs (e.g., broad H α , strong optical FeII emission, etc.), have to be explained by a starburst alone. The variability in one of the absorption-line systems (Boroson et al 1991; Kollatschny, Dietrich & Hagen 1992) and nonthermal radio continuum (Condon et al 1991) does not favour this hypothesis but a compact single object, i.e., AGN. The dominance of a nonstellar source in the near-IR band is also suggested from the very weak CO absorption band (Majewski et al 1993; Ridgway et al 1994; Shier et al 1996). Therefore there are many difficulties to explain without a powerful AGN.

(ii) Small-scale occultation and reflection of a central source

The weak X-ray luminosity could be explained by a reflection-dominated object. A similar 2–10 keV X-ray luminosity to that of NGC6240 implies that the intrinsic luminosity of the hidden central source would be as large as 10^{45} erg s $^{-1}$. This hypothesis is, however, inconclusive without detection of a strong Fe K line, and the apparent Seyfert 1 nature needs explanation. The loose upper limit on the EW of the Fe K line (< 1 keV) cannot rule out this possibility.

In this hypothesis, the central source must be absorbed completely even in the X-ray band. However, the reddening implied for the UV/optical continuum ($A_V \sim 2$, Boksenberg et al 1977; Hamilton & Keel 1987; Smith et al 1995) is far too small. To hide only a central X-ray source behind the optically thick matter, the obscuration must occur on very small scale (well inside the broad line region). The variability time scale (a few years) of the absorption system (Boroson et al 1991) suggests that the inner 1pc of the nucleus is seen. Since X-ray emission appears to be generated within 10 Schwarzschild radii ($< 10^{-4}$ pc for a $10^8 M_\odot$ black hole), the occultation has to occur on scales between 10^{-4} pc to 1 pc. Disk warping (Maloney, Begelman & Pringle 1996) may be responsible for this, although how a large column density in the line of sight can be achieved is uncertain.

(iii) An X-ray quiet central source

Assuming that we are seeing an intrinsically X-ray quiet QSO nucleus through moderate obscuration by low ionization gas, may be a straightforward explanation. BAL QSOs have been recognized as significantly weak soft X-ray sources from ROSAT observations (Green & Mathur 1996). Whether it is due to large absorption or low luminosity intrinsic to the central sources is still uncertain (Mushotzky 1997), although there is one example showing that absorption seems to be the case (Mathur, Elvis & Singh 1995). If the hard X-ray emission detected with ASCA is the direct radiation from the nucleus, the X-ray source in Mrk231 would be intrinsically X-ray quiet ($L_{2-10\text{keV}} \simeq 2 \times 10^{42}$ erg s $^{-1}$) as well as being absorbed ($N_H \sim 2 \times 10^{22}$ cm $^{-2}$, see Table 4).

This X-ray quiet hypothesis would also bring a serious problem with the X-ray heating (photoionization) model of FeII (e.g., Netzer 1987; Collin-Souffrin et al 1988). The intrinsic deficit of hard X-ray photons fails to explain the fact that Mrk231 is one of the ‘extreme FeII emitters’ ($\text{FeII}/\text{H}\beta \approx 2.1$, Lipari 1994). The correlation between soft X-ray slope and $\text{EW}(\text{FeII})$ found by Wilkes, Elvis & McHardy (1987) using the data from the Einstein Observatory is also in the opposite sense to the standard photoionization model.

In order to provide sufficient ionizing UV photons to account for the observed large luminosities of Balmer lines and the optical–UV continuum, a large excess in the UV–soft X-ray band, which would however be unobservable because of the moderate absorption, is required. This is possibly related to the class of ultrasoft AGNs (or narrow-line Seyfert 1s, Boller, Brandt & Fink 1996) which, too, often show strong FeII emission.

Alternatively, the bulk of the energy for the optical/UV emission may be supplied from a starburst and mechanical heating by the starburst wind is responsible for the FeII excitation, as proposed by Lipari, Colina & Macchetto (1994) and Lipari, Terlevich & Macchetto (1993).

6.3 The large far-IR excess in Arp220

The energy distribution of the Arp220 is characterized by the enormous far-IR excess, which places the galaxy at the early stage of the evolution scenario of infrared galaxies proposed by Sanders et al (1988). The lack of direct evidence for a QSO-like central source favours a powerful, young starburst as the major source of the bolometric luminosity. A handful of hints of AGN activity, the high $[\text{OIII}]/\text{H}\beta$ ratio in the nucleus (Sanders et al 1988) and a compact radio core (Lonsdale, Smith & Lonsdale 1995) can be reconciled with photoionization by hot stars (e.g., ‘warmer’, Terlevich & Melnick 1985) and a cluster of radio supernovae (Smith, Lonsdale & Lonsdale 1998), respectively. A highly obscured starburst can account for the ‘ionizing photon deficit’ problem (DePoy et al 1987; Leitherer & Heckman 1995; Armus et al 1995).

No detection of strong hard X-ray emission (> 5 keV) fails to provide any evidence for a powerful AGN. However, this does not readily rule out the possibility of a deeply buried AGN as a major source of the far-IR luminosity, because the starburst in Arp220 does not appear to be sufficiently powerful, as discussed below.

The observed $\text{H}\alpha$ and soft X-ray emission in Arp220 are consistent with the superwind scenario (Heckman et al 1996; Section 6.1.1). Importantly, in the superwind model, the luminosity of the nebular emission depends on the mechanical luminosity of starburst winds. Therefore the soft X-ray and $\text{H}\alpha$ emission in Arp220, one order of magnitude less luminous than NGC6240, may suggest that the starburst taking place in Arp220 is much weaker than in NGC6240 despite the larger far-IR luminosity. This speculation is consistent with the conclusion of Scoville et al (1997), based on the weak mm-waveband free-free emission where dust is no longer optically thick.

A possible explanation for the weak mechanical luminosity can be found if an upper mass cut-off (say, at $30M_\odot$) in the initial mass function (IMF) is assumed. This argu-

ment has also been discussed for the ionizing photon deficit problem. The absence of a population of massive stars would result in a smaller kinetic energy of the starburst wind which is provided predominantly by Type II supernovae and Wolf-Rayet (WR) stars while low mass stars power the far-IR luminosity. Few WR stars, that evolve from O stars with an initial mass of larger than $20\text{--}40 M_\odot$, would exist. The lack of WR feature (at $\lambda \sim 4660\text{\AA}$) in the optical spectrum is consistent with this. Recombination lines from HII regions would also remain weak because of fewer ionizing stars (stars with $M \geq 20M_\odot$). The rather ‘tepid’ IRAS colour agrees with the dominance of low mass stars as a primary heating source of the far-IR emission, since dust grains heated by such population of stars mainly contribute to the IRAS $60\mu\text{m}$ and $100\mu\text{m}$ range (Mouri & Taniguchi 1992).

Although this idea of a truncated IMF may partly solve the problem, the star formation rate estimated from the far-IR luminosity still overproduces the mechanical luminosity by a factor of ~ 5 more than needed to account for the observed soft X-ray/ $\text{H}\alpha$ luminosities (Heckman et al 1996). We therefore conclude that the starburst in Arp220 is less powerful than the other FIRGs in terms of the mechanical luminosity.

A deeply buried starburst ($A_V \sim 50$, Sturm et al 1996) inferred from the ISO spectroscopy is not seen in the X-ray data. The column density $N_{\text{H}} \sim 1 \times 10^{23} \text{ cm}^{-2}$, deduced from $A_V \sim 50$ is no longer opaque in the hard X-ray band (e.g., > 3 keV). However, no hard X-ray emission expected from such an obscured starburst is detected in the ASCA spectrum. The observed 2–10 keV luminosity of Arp220 (Table 7) is a factor of 6 smaller than that scaled from the luminosity of M82 using the far-IR luminosity. At least the X-ray data do not verify a starburst in a heavy ($A_V \sim 50$) obscuration to be particularly powerful.

If the far-IR emission of Arp220 is instead powered by an AGN, it must be a Compton-thick source. Because of their faintness in X-ray, Compton-thick AGNs are usually hard to detect. Only nearby objects like NGC1068 were detectable in the past X-ray surveys. However, such sources appear to be common. A recent BeppoSAX survey has found a number of Compton-thick Seyfert 2s (Salvati et al 1997). The other far-infrared excess galaxies such as NGC4945 (Iwasawa et al 1993; Done et al 1996), the Circinus galaxy (Matt et al 1996) and NGC6240 (Iwasawa & Comastri 1998) also contain AGNs hidden behind obscuration with $N_{\text{H}} > 10^{24} \text{ cm}^{-2}$. A difference between these Compton-thick sources and Arp220 would be the covering factor of the obscuration. No detection of even the reflection-dominated X-ray spectrum means a central X-ray source to be covered by an extremely thick matter almost completely. Very little hot dust irradiated by a central AGN would then be visible, which is consistent with the cool characteristic temperature of the far-IR emission in the IRAS band. Therefore a starburst taking place at the smaller optical depth ($\tau_{\text{dust}} \sim 1$, or $A_V \sim 50$) would dominate the spectrum from near-IR to mid-IR as observed.

6.4 Implications for other ultraluminous galaxies

The far-IR dominance in the spectral energy distribution is similar between FIRGs and Seyfert 2 galaxies. There are indications that starbursts can be a significant energy source

in Seyfert 2 galaxies (Heckman et al 1995, 1997) and the outer parts of the obscuring matter of AGNs may be the place where the starbursts are occurring. Perhaps powerful FIRGs are even more heavily obscured version of Seyfert 2s. Starbursts appear to dominate the emission of FIRGs in the near-IR to mid-IR band. However, the optical depth to the starburst regions is still small compared with that to the hidden X-ray sources in some FIRGs (NGC6240, NGC4945). Arp220 might also be the case. When the obscuration of a central source is not thick enough (say, a few times of 10^{23}cm^{-2} in N_{H}), AGN features would emerge in the optical–mid-IR spectrum (Mrk273).

Some ultraluminous IR galaxies (ULIRGs) with a clear Seyfert-2 optical spectrum or polarized broad-line region have been found to harbour an absorbed X-ray source with N_{H} values of order of 10^{23}cm^{-2} (Mrk273, this work; Mrk463E, Ueno et al 1996; IRAS20460+1925, Ogasaka et al 1997; IRAS23060+0505, Brandt et al 1997). They can be considered as luminous versions of classical Seyfert 2 galaxies. However, no significant X-ray detection has been reported for hyperluminous galaxies at higher redshift, like IRAS F15307+3252 (Fabian et al 1996; Ogasaka et al 1997) and IRAS F10214+4724 (no detection with 80 ks ASCA observations while 2σ detection with ROSAT reported by Lawrence et al 1994) despite clear Seyfert-2 characteristics of their optical emission-line spectra (Cutri et al 1994; Rowan-Robinson et al 1991; Serjeant et al 1998). No detection, at least in the ROSAT band, has been reported for a further four hyperluminous galaxies, IRAS F00235+1024, F12514+1027, F14481+4454 and F1537+1950 (Wilman et al 1998). For IRAS P09104+4109 (Kleinmann et al 1988), cluster emission surrounding the hyperluminous galaxy dominates the observed X-rays ($2 \times 10^{45}\text{erg s}^{-1}$, Fabian & Crawford 1995).

The lack of strong hard X-ray emission in hyperluminous galaxies poses the same problem as with Arp220. If a powerful AGN exists, only faint scattered light would be emitted and the upper limit of the $L(2\text{--}10\text{keV})/L(\text{FIR})$ ratio for IRAS F15307+3252 (4×10^{-3} , Ogasaka et al 1997) is still consistent with the known cases of NGC1068 and NGC6240 for which the ratio is $\sim 10^{-3}$. If an AGN is intrinsically weak, a central massive black hole may not have grown enough to emit QSO luminosity while a powerful starburst provide the bulk of the bolometric luminosity, which would explain the X-ray quiet nature.

Fabian et al (1998) has proposed a nearly spherical obscuring geometry on 100 pc scale rather than a pc scale toroidal one for the major contributors to the X-ray background (XRB). ULIRGs may be extreme cases of much larger column density. Primary obscuration of a central X-ray source (e.g., $N_{\text{H}} \gg 10^{24}\text{cm}^{-2}$) perhaps occurs at small radii (≤ 1 pc) otherwise total mass becomes exceedingly large while molecular gas clouds, composing a moderate obscuration on hundreds pc scale, absorb the radiation escaping from the inner region. The small opening fraction of the large-scale absorbing shroud makes the scattered light weak. It should be noted that a high covering fraction of obscuration is demanded to explain the XRB with the obscured AGN models (Setti & Woltjer 1989; Madau, Ghisellini & Fabian 1994; Celotti et al 1995; Comastri et al 1995).

ACKNOWLEDGEMENTS

KI thank all the member of the ASCA team who operate the satellite and maintain the software and database. A.C. Fabian, Y. Taniguchi and the referee are thanked for helpful comments. J. Hibbard is thanked for information on his unpublished observation. The ASCA observations were made by following PIs: T. Nakagawa (Mrk273 and NGC6240), L. Armus (Mrk231) and the ASCA team (Arp220). This research has made use of data obtained through the High Energy Astrophysics Science Archive Research Center (HEASARC), provided by NASA's Goddard Space Flight Center. KI thank PPARC for support.

REFERENCES

Antonucci R.R.J., Miller J.S., 1985, *ApJ*, 297, 621
 Armus L., Heckman T.M., Miley G.K., 1990, *ApJ*, 364, 471
 Armus L., Surace J.A., Soifer B.T., Matthews K., Graham J.R., Larkin J.E., 1994, *AJ*, 108, 76
 Armus L., Shupe D.L., Matthews K., Soifer B.T., Neugebauer G., 1995, *ApJ*, 440, 200
 Baan W.A., 1985, *Nat*, 315, 26
 Boksenberg A., Carswell R.F., Allen D.A., Fosbury R.A.E., Penston M.V., Sargent W.L.W., 1977, *MNRAS*, 178, 451
 Boller Th., Brandt W.N., Fink H.H., 1996, *A&A*, 305, 53
 Boroson T.A., Meyerts K.A., Morris S.L., Persson S.E., 1991, *ApJ*, 370, L19
 Braatz J.A., Wilson A.S., Henkel C., 1996, *ApJS*, 106, 51
 Brandt W.N., Iwasawa K., Reynolds C.S., 1996, *MNRAS*, 281, L41
 Brandt W.N., Fabian A.C., Takahashi K., Fujimoto R., Yamashita A., Inoue H., Ogasaka Y., 1997, *MNRAS*, 290, 617
 Bryant P.M., Scoville N.Z., 1996, *ApJ*, 457, 678
 Celotti A., Fabian A.C., Ghisellini G., Madau P., 1995, *MNRAS*, 277, 1169
 Chevalier R.A., Clegg A.W., 1985, *Nat*, 317, 44
 Collin-Souffrin S., Hameury J., Joly M., 1988, *A&A*, 205, 19
 Comastri A., Setti G., Zamorani G., Hasinger G., 1995, *A&A*, 296, 1
 Comastri A., Vignali C., Cappi M., Matt G., Audano R., Awaki H., Ueno S., 1997, *MNRAS*, 295, 443
 Condon J.J., Frayer D.T., Broderick J.J., 1991, *AJ*, 101, 362
 Condon J.J., Huang Z.-P., Yin Q.F., Thuan T.X., 1991, *ApJ*, 278, 65
 Cutri R.M., Huchra J.P., Low F.J., Brown R.L., van den Bout P.A., 1994, *ApJ*, 424, L65
 Dahlem M., Petr M.G., Lehnert M.D., Heckman T.M., Ehle M., 1997, *A&A*, 320, 731
 David L.P., Jones C., Forman W., 1992, *ApJ*, 388, 82
 DeGrijp M.H.L., Keel W.C., Miley G.K., Goudfrooij P., Lub J., 1992, *A&AS*, 96, 389
 DePoy D., Becklin E., Wynn-Williams C.G., 1986, *ApJ*, 307, 116
 DePoy D., Becklin E., Geballe T., 1987, *ApJ*, 316, L63
 Dermer C.D., Bland-Hawthorn J., Chiang J., McNaron-Brown K., 1997, *ApJ*, 484, L121
 Dickey J.M., Lockman F.G., 1990, *ARA&A*, 28, 215
 Done C., Madejski G.M., Smith D.A., 1996, *ApJ*, 463, L63
 Dos Santos P.M., Lepine J.R.D., 1979, *Nat*, 278, 34
 Doyon R., Wells M., Wright G.S., Joseph R.D., Nadeau D., James P.A., 1994, *ApJ*, 437, L23
 Dudley C.C., Wynn-Williams C.G., 1997, *ApJ*, 488, 720
 Eales S.A., Arnaud K.A., 1988, *ApJ*, 324, 193
 Fabbiano G., 1988, *ApJ*, 330, 672
 Fabian A.C., Crawford C.S., 1995, *MNRAS*, 274, L75

Fabian A.C., Cutri R.M., Smith H.E., Crawford C.S., Brandt W.N., 1996, MNRAS, 283, L95

Fabian A.C., Barcons X., Almaini O., Iwasawa K., 1998, MNRAS, 297, L11

Feldman U., 1992, *Physica Scripta*, 46, 202

Gallimore J.F., Baum S.A., O'Dea C.P., 1997, *Nat*, 388, 852

Genzel R., et al, 1998, *ApJ*, 498, 579

Goldader J.D., Joseph R.D., Doyon R., Sanders D.B., 1995, *ApJ*, 444, 97

Graham J.R., Carico D.P., Matthews K., Soifer B.T., Wilson T.D., 1990, *ApJ*, 354, L5

Green P., Mathur S., 1996, *ApJ*, 462, 637

Greenhill L.J., Gwinn C.R., Antonucci R., Barvainis R., 1996, *ApJ*, 472, L21

Greenhill L.J., Moran J.M., Herrnstein J.R., 1997, *ApJ*, 481, L23

Hamilton D., Keel W.C., 1987, *ApJ*, 321, 211

Heckman T.M., Armus L., Miley G.K., 1987, *AJ*, 92, 276

Heckman T.M., Armus L., Miley G.K., 1990, *ApJS*, 74, 833

Heckman T., et al, 1995, *ApJ*, 452, 549

Heckman T.M., Dahlem M., Eales S.A., Fabbiano G., Weaver K.A., 1996, *ApJ*, 457, 616

Heckman T.M., Gonzalez-Delgado R., Leitherer C., Meuer G.R., Krolik J.H., Wilson A.S., Koratkar A., Kinney A., 1997, *ApJ*, 482, 114

Helfer T.T., Blitz L., 1995, *ApJ*, 450, 90

Huchings J.B., Neff S.G., 1987, *AJ*, 92, 14

Iwasawa K., Koyama K., Awaki H., Kunieda H., Makishima K., Tsuru T., Ohashi T., Nakai N., 1993, *ApJ*, 409, 155

Iwasawa K., Yaqoob T., Awaki H., Ogasaka Y., 1994, *PASJ*, 46, L167

Iwasawa K., 1995, PhD thesis, Nagoya University, Nagoya

Iwasawa K., Fabian A.C., Matt G., 1997, *MNRAS*, 289, 443

Iwasawa K., Fabian A.C., Ueno S., Awaki H., Fukazawa Y., Matsushita K., Makishima K., 1997, *MNRAS*, 285, 683

Iwasawa K., Comastri A., 1998, *MNRAS*, 297, 1219

Jackson J.M., Poglione T.A.D., Ishizuki S., Nguyen Q.R., 1993, *ApJ*, 418, L13

Kii T., Nakagawa T., Fujimoto R., Ogasaka T., Miyazaki T., Kawabe R., Terashima Y., 1997, *X-Ray Imaging and Spectroscopy of Cosmic Hot Plasma*, eds F. Makino and K. Mitsuda, Universal Academy Press, Tokyo, p161

Kleinmann S.G., Hamilton D., Keel W.C., Wynn-Williams C.G., Eales S.A., Becklin E.E., Kuntz K.D., 1988, *ApJ*, 328, 161

Knappen J.H., Laine S., Yates J.A., Robinson A., Richards A.M.S., Doyon R., Nadeau D., 1997, *ApJ*, 490, L29

Kollatschny W., Dietrich M., Hagan H., 1992, *A&A*, 264, L5

Komossa S., Schulz H., Greiner J., 1998, *A&A*, 334, 110

Koski A.T., 1978, *ApJ*, 223, 56

Koyama K., Inoue H., Tanaka Y., Awaki H., Takano S., Ohashi T., Matsuoka M., 1989, *PASJ*, 41, 731

Lawrence A., Rigopoulou D., Rowan-Robinson M., McMahon R.G., Broadhurst T., Lonsdale C.J., 1994, *MNRAS*, 266, L41

Leitherer C., Heckman T.M., 1995, *ApJS*, 96, 9

Lester D.F., Carr J.S., Joy M., Gaffney N., 1990, *ApJ*, 352, 544

Lipari S., Colina L., Macchetto F., 1994, *ApJ*, 427, 174

Lipari S., 1994, *ApJ*, 436, 102

Lipari S., Terlevich R., Macchetto F., 1993, *ApJ*, 406, 451

Lonsdale C.J., Helou G., Good J.C., Rice W., 1985, Catalogued Galaxies and Quasars Observed in the IRAS Survey (Pasadena: JPL)

Lonsdale C.J., Smith H.E., Lonsdale C.J., 1995, *ApJ*, 438, 632

Lutz D., et al 1996, *A&A*, 315, L137

Madau P., Ghisellini G., Fabian A.C., 1994, *MNRAS*, 270, 17

Magdziarz P., Zdziarski A.A., 1995, *MNRAS*, 273, 837

Majewski S.R., Hereld M., Koo D.C., Illingworth G.D., Heckman T.M., 1993, *ApJ*, 402, 125

Maloney P.R., Begelman M.C., Pringle J.E., 1996, *ApJ*, 472, 582

Mariani S., et al 1998, in L. Scarsi, H. Bradt, P. Giommi and F. Fiore, eds, *Active X-ray Sky: Results from BeppoSAX and Rossi-XTE*, Kluwer, in press

Marshall F.E., Netzer H., Arnaud K.A., Boldt E.A., Holt S.S., Jahoda K.M., Kelley R., Mushotzky R.F., 1993, *ApJ*, 405, 168

Mathur S., Elvis M., Singh K.P., 1995, *ApJ*, 455, L9

Matt G., Piro L., Antonelli L.A., Fink H.H., Meurs E.J.A., Perola G.C., 1994, *A&A*, 292, L13

Matt G., et al 1996, *MNRAS*, 281, L69

Matt G., et al 1997, *A&A*, 325, L13

McCarthy P.J., Heckman T.M., van Breugel W., 1987, *AJ*, 92, 264

Miller J.S., Goodrich R.W., Mathews W.G., 1991, *ApJ*, 378, 47

Mitsuda K., 1995, in H. Böhringer, G.E., Morfill, J. Trümper, eds, 17th Texas Symposium, NY. Acad. Sci., New York, p213

Moran E.C., Lehnert M.D., 1997, *ApJ*, 478, 172

Morrison R., McCammon D., 1983, *ApJ*, 270, 119

Mouri H., Taniguchi Y., 1992, *ApJ*, 386, 68

Mushotzky R.F., 1997, in 'Mass Ejection from AGN', (astro-ph/9705004)

Nakai N., 1989, *PASJ*, 41, 1107

Neff S.G., et al 1994, *ApJ*, 430, 545

Netzer H., 1987, *MNRAS*, 225, 55

Nezter H., Turner T.J., George I.M., 1998, *ApJ*, in press

Ogasaka Y., Inoue H., Brandt W.N., Fabian A.C., Kii T., Nakagawa T., Fujimoto R., Otani C., *PASJ*, 49, 179

Piccinotti G., Mushotzky R.F., Boldt EA., Holt S.S., Marshall F.E., Serlemitsos P.J., Shafer R.A., 1982, *ApJ*, 253, 485

Pier E.A., Antonucci R., Hurt T., Kriss G., Krolik J., 1994, *ApJ*, 428, 124

Ptak A., Serlemitsos P.J., Yaqoob T., Mushotzky R.F., 1997, *AJ*, 113, 1286

Reynolds C.S., 1997, *MNRAS*, 286, 513

Ridgeway S.E., Wynn-Williams C.G., Becklin E.E., 1994, *ApJ*, 428, 609

Rieke G.H., Lebofsky M.J., Thompson R.I., Low F.J., Tokunaga A.T., 1980, *ApJ*, 238, 24

Rieke G., 1988, *ApJ*, 331, L5

Rigopoulou D., Lawrence A., Rowan-Robinson M., 1996, *MNRAS*, 278, 1049

Rigopoulou D., et al, 1998, in preparation

Roche P.F., Aitken D.K., Whitmore B., 1983, *MNRAS*, 265, 486

Rowan-Robinson M., et al, 1991, *Nat*, 351, 719

Rush B., Malkan M.A., Fink H.H., Voges S.W., 1996, *ApJ*, 471, 190

Salvati M., Bassani L., Della Ceca R., Maiolino R., Matt G., Zamorani G., 1997, *A&A*, 323, L1

Sanders D.B., Mirabel I.F., 1996, *ARAA*, 34, 749

Sanders D.B., Scoville N.Z., Soifer B.T., 1991, 370, 158

Sanders D.B., Soifer B.T., Elias J.H., Madore B.F., Matthews K., Neugebauer G., Scoville N.Z., 1988, *ApJ*, 325, 74

Schmidt G.D., Miller J.S., 1985, *ApJ*, 290, 517

Schulz H., Komossa S., Berghöfer T., Boer B., 1998, *A&A*, 330, 823

Scoville N.Z., Sargent A.I., Sanders D.B., Soifer B.T., 1991, *ApJ*, 366, L5

Scoville N.Z., Yun M.S., Bryant P.M., 1997, *ApJ*, 484, 702

Scoville N.Z., et al, 1998, *ApJ*, 492, L107

Serjeant S., Rawlings S., Lacy M., McMahon R.G., Lawrence A., Rowan-Robinson M., Mountain M., 1998, *MNRAS*, 298, 321

Serlemitsos P.J. et al, 1995, *PASJ*, 47, 105

Setti G., Woltjer I., 1989, *A&A*, 224, L21

Shier L.M., Rieke M.J., Rieke G.H., 1996, *ApJ*, 470, 222

Smith H.E., Lonsdale C.J., Lonsdale C.J., 1998, *ApJ*, 492, 137

Smith P.S., Schmidt G.D., Allen R.G., Angel J.R.P., 1995, *ApJ*, 444, 146

Soifer B.T., et al, 1984, *ApJ*, 278, L71

Soifer B.T., Sanders D.B., Madore B.F., Neugebauer G., Daniel-

son G.E., Elias J.H., Lonsdale C.J., Rice W.L., 1987, *ApJ*, 320, 238

Solomon P.M., Downes D., Radford S.J.E., 1992, *ApJ*, 387, L55

Strickland D.K., Ponman T.J., Stevens I.R., 1997, *A&A*, 320, 378

Sturm E., et al, 1996, *A&A*, 315, L133

Surace J.A., Sanders D.B., Vacca W.D., Veilleux S., Mazzarella J.M., 1998, *ApJ*, 492, 116

Tacconi L.J., Genzel R., Blietz M., Cameron M., Harris A.I., Madsen S., 1994, *ApJ*, 426, L77

Tanaka Y., Inoue H., Holt S.S., 1994, *PASJ*, 46, L37

Telesco C.M., Becklin E.E., Wynn-Williams C.G., Harper D.A., 1984, *ApJ*, 282, 427

Terlevich R., Melnick J., 1985, *MNRAS*, 213, 841

Thompson I., Stockman H.S., Angel J.R.P., Beaver E.A., 1980, *MNRAS*, 192, 53

Thronson H.A., Majewski S., Descartes L., Hereld M., 1990, *ApJ*, 364, 456

Tomisaka K., Ikeuchi S., 1988, *ApJ*, 330, 695

Tsuru T., Awaki H., Koyama K., Ptak A., 1997, *PASJ*, 49, 619

Turner T.J., George I.M., Nandra K., Mushotzky R.F., 1997, *ApJS*, 113, 23

Turner T.J., Urry C.M., Mushotzky R.F., 1993, *ApJ*, 418, 653

Ueno S., Mushotzky R.F., Koyama K., Iwasawa K., Awaki H., 1994, *PASJ*, 46, L71

Ueno S., Koyama K., Awaki H., Hayashi I., Blanco P.R., 1996, *PASJ*, 48, 389

van der Werf P.P., Genzel R., Krabbe A., Blietz M., Lutz D., Drapatz S., Ward M.J., Forbes D.A., 1993, *ApJ*, 405, 522

Walker C.E., Lebofsky M.J., Rieke G.H., 1988, *ApJ*, 325, 687

Wang T., Brinkmann W., Bergeron J., 1996, *A&A*, 309, 81

Ward M.J., Done C., Fabian A.C., Tennant A.F., Shafer R.A., 1988, *ApJ*, 324, 767

Weaver K.A., Nousek J., Yaqoob T., Mushotzky R.F., Makino F., Otani C., 1996, *ApJ*, 458, 160

Weedman D.W., 1973, *ApJ*, 183, 29

Whiteoak J.B., Gardner F.F., 1978, *PASA*, 3, 5

Wilkes B.J., Elvis M., McHardy I., 1987, *ApJ*, 321, L23

Wilman R.J., Fabian A.C., Cutri R.M., Crawford C.S., Brandt W.N., 1998, *MNRAS*, submitted

Wilson A.S., Elvis M., 1997, *Ap&SS*, 248, 167

Wilson A.S., Elvis M., Lawrence A., Bland-Hawthorn J., 1992, *ApJ*, 391, L75

Xia X.-Y., Boller Th., Wu H., Deng Z.-G., Gao Y., Zou Z.-L., Mao S., Börner G., 1998, *ApJ*, 496, L9